

POLITECNICO DI TORINO

Master's Degree in communication and computer
networks engineering



Master's Degree Thesis

Design and Implementation of a 3D Indoor Localization System Enabling Augmented Reality Applications

Supervisors

Prof. Roberto GARELLO

Eng. Francesco SOTTILE

Eng. Luigi CORIASCO

Candidate

Shiva EHSANIBALAJORSHARY

April 2021

Summary

This thesis presents design and implementation of a UWB 3-D localization system for real time augmented reality applications to be applied in TV studios. It first presents the state of art of RTLS based on the UWB technology. After that, it focuses on the design of the RTLS. The UWB-based Localization System is formed by the Anchors and the Tags. In a real-time location system (RTLS), anchors are electronic devices that detect UWB pulses emitted by UWB Tags and forward them to the location server for calculating tag positions. Tags are small electronic devices that are attached to objects that need to be tracked. These devices exchange range messages and send in real-time the range measurements to a gateway where a localization algorithm, based on EKF, runs to estimate tag's position according to a relative references system. In this thesis, to evaluate the performance of the designed EKF algorithm, 25 test points have been chosen for the tag's position and the localization algorithm has been tested via Matlab simulation in an indoor area where 8 anchors have been deployed. Measurements campaign have been carried out in RAI by using UWB devices from synchronicIT and these measurements were done in different scenarios without obstacle and with human body. The positioning phase was used the extended Kalman filter (EKF) since it is robust and less complex than many others algorithms. In this thesis, EKF is simulated to show its features and how its parameters change the tracking performance by using two different state namely, Position (P) model and Position velocity (PV) model and several tests were done in order to evaluate and compare different localization performance without obstacle and with human body. It was found that the localization depends on the precision of ranging measurements and with more ranging measurements the system becomes more precise. Due to human body interference, sometimes the direct path is obstructed and the receiver synchronizes on a reflected path, thus affecting the range measurement. In this thesis, We start with 1 tag and evaluate the performance to find the best σ (which is one of parameters of Q matrix) that minimise the 3DLoc error rmse for two state models, P model and PV model. Then we continue this simulation by having 2 tags and 3 tags on human body to see how performance will be changed.

Acknowledgements

In first place, I would like to express my deep and sincere gratitude to Professor Garello for giving me this opportunity to have this thesis under his supervision, and Eng. Francesco Sottile for his constant guidance and assistance and immense knowledge. Special thanks to my brother Roozbeh who trust on my capabilities, for believing in me and knowing my future is brightened. Finally, I would like thank to my parents and my brother kaveh for caring and supporting me in all my choices and decisions.

Table of Contents

List of Tables	IX
List of Figures	X
Acronyms	XIII
1 Introduction	1
1.1 Real-Time Locating System Applications	1
1.2 Objective of Thesis	2
1.3 Overview of Thesis	2
2 Overview of Indoor Localization systems	4
2.1 Introduction	4
2.2 Ranging Techniques	5
2.2.1 RSSI	6
2.2.2 OW-ToA	6
2.2.3 TW-ToA	7
2.3 Localization Algorithms	8
2.3.1 KF	9
2.3.2 EKF	9
3 Ranging Measurements Campaign for 3D Localization	11
3.1 Introduction	11
3.2 Deployment of the UWB Localisation System	11
3.3 Distance Measurement Scenarios	13
3.4 Ranging Performance Evaluation	15
3.4.1 Without Obstacle	16
3.4.2 With Human body	18
4 Design and Evaluation of the 3D Localization Algorithm - 1 Tag	22
4.1 Design of the EKF for 3D Localization for 1 Tag	22

4.1.1	State Models	22
4.1.2	Measurement model	24
4.2	Evaluation of Localization Performance and Optimization	25
4.2.1	Static Condition without Obstacles	25
4.2.2	Static Condition with Human Body – 1 Tag on the right shoulder	31
4.2.3	Dynamic Condition with Human Body – Tag on the right shoulder (walk)	35
4.2.4	Dynamic Condition with Human Body – Tag on the right shoulder (run)	36
4.2.5	Dynamic Condition with Human Body – Tag on the pocket (walk)	38
4.2.6	Dynamic Condition with human Body – Tag on the pocket (run)	40
4.2.7	Dynamic Condition with Human Body – Tag on the back belt (walk)	42
4.2.8	Dynamic Condition with Human Body – Tag on the back belt (run)	44
5	Design and Evaluation of the 3D Localization Algorithm - 2 Tags	47
5.1	Design of the EKF for 3D Localization for 2 Tags	47
5.1.1	State Models	47
5.1.2	Measurement Model	48
5.2	Evaluation of the Localization Performance and Optimization	49
5.2.1	Static Condition with Human Body – 2 Tags on the right shoulder	50
5.2.2	Static Condition with Human Body – 2 Tags on the Pocket	51
5.2.3	Static Condition with Human Body – 2 Tags on the Back Belt	52
6	Design and Evaluation of the EKF for 3D Localization - 3 Tags	55
6.1	Design of the EKF for 3D Localization for 3 Tags	55
6.1.1	State Models	55
6.1.2	Measurement Model	56
6.2	Evaluation of the Localization Performance and Optimization	58
6.2.1	Static Condition with Human Body – Tag on the Shoulder	58
6.2.2	Static Condition with Human Body – Tag on the Pocket	60
6.2.3	Static Condition with Human Body – Tag on the Back Belt	61
7	Performance Comparisons and Conclusions	64
7.1	Performance Comparisons	64
7.2	Conclusions	64

Appendix	68
.1 Main code	68
.2 P model and PV model for 3 Tags	69
.3 EKF for 3 Tags	70
Bibliography	71

List of Tables

3.1	Global statistics for ranging with Tripod	18
3.2	Global statistics for ranging with Human body	20
4.1	Performance of $\sigma_a = 5$ for P model	26
4.2	Performance of $\sigma_a = 5$ for PV model	30
4.3	Performance of $\sigma_a = 0.01$ for P model	34
5.1	2 Tags - Performance of σ_a for P model	50
5.2	2 Tags - Performance of σ_a for PV model	51
5.3	2 Tags - Performance of σ_a for P model	52
5.4	2 Tags - Performance of σ_a for PV model	53
6.1	3 Tags - Performance of σ_a for P model	59
6.2	3 Tags - Performance of σ_a for PV model	60
6.3	3 Tags - Performance of σ_a for P model	61
6.4	3 Tags - Performance of σ_a for PV model	62
7.1	Comparison effect of human body on UWB signal by having different number of Tags	64

List of Figures

2.1	One example of Zigbee	5
2.2	Temporal diagram for one way ToA	7
2.3	Temporal diagram for two way ToA	8
3.1	Tag - size 4.6 x 7.3 cm	12
3.2	Anchor - size 9.8 x 9.8 cm	12
3.3	Test points	12
3.4	Tripod - height 93 cm and height 153 cm	13
3.5	Back belt - height 93 cm	13
3.6	Right pocket - height 77 cm	14
3.7	Right shoulder - height 156 cm	14
3.8	4 orientation of Human body Ranging Localization	14
3.9	Error along the axes	15
3.10	Static Ranging Localization	16
3.11	Ranging without obstacles (h = 93 cm), (Test Point 0)	17
3.12	Ranging without obstacles (h = 153 cm), (Test Point 0)	17
3.13	Multi-Path Effect	18
3.14	Ranging with right shoulder (h=156 cm),(Test Point 0)	19
3.15	Ranging with Human body (tag on the back belt h = 111 cm)	19
3.16	Ranging with Human body (tag inside the right pocket h = 77 cm)	20
3.17	The Multi-Path effect in the presence of the Human body	21
4.1	Test point 0 - 3DLocErr [avg=0.049, std=0.017, RMS=0.052]m	26
4.2	Ratio between σ_a and rmse as a function of σ_a	27
4.3	P model for 1 Tag - without obstacle (153cm)	27
4.4	Test point 0 - 3DLocErr [avg=0.050, std=0.026, RMS=0.057] m	28
4.5	Ratio between σ_a and rmse as a function of σ_a	29
4.6	Global error of PV model for 1 tag - without obstacle(153 cm)	29
4.7	P model - 1 Tag on the right shoulder - Test point 0	31
4.8	P model - 1 Tag on the right shoulder	32
4.9	PV model - 1 Tag on the right shoulder	32

4.10	PV model - 1 Tag on the right shoulder	33
4.11	P model - 1 Tag on the right shoulder	33
4.12	$\sigma_a = 4$, P model, walking by having 1 tag on right shoulder	35
4.13	$\sigma_a = 1.5$, PV model, walking by having 1 tag on right shoulder	36
4.14	$\sigma_a = 4$, P model, tag on right shoulder while running	37
4.15	$\sigma_a = 1.5$, PV model in case of running by having 1 tag on right shoulder	38
4.16	$\sigma_a = 4$, P model, walking by having 1 tag on the pocket	39
4.17	$\sigma_a = 1.5$, PV model, walking by having 1 tag on the pocket	40
4.18	$\sigma_a = 4$, P model, running by having 1 tag on pocket	41
4.19	$\sigma_a = 1.5$, PV model, running by having 1 tag on pocket	42
4.20	$\sigma_a=4$, P model, walking by having 1 tag on back belt	43
4.21	$\sigma_a = 1.5$, PV model, walking by having 1 tag on back belt	44
4.22	$\sigma_a = 4$, P model, running by having 1 tag on back belt	45
4.23	$\sigma_a = 1.5$, PV model, running by having 1 tag on back belt	46
5.1	P model - ratio σ_a and rmse	50
5.2	P model - 2 Tags on right shoulder	51
5.3	PV model - 2 Tags on right shoulder	52
5.4	P model - 2 Tags on back belt	53
5.5	PV model - 2 Tags on back belt	54
6.1	P model - 3 Tags on right shoulder	59
6.2	PV model - 3 Tags on right shoulder	60
6.3	Ratio between σ_a and rmse as a function of σ_a	61
6.4	P model - 3 Tags on back belt	62
6.5	Ratio between σ_a and rmse as a function of σ_a	63
6.6	PV model - 3 Tags on back belt	63
7.1	Measurements Scenarios	65
7.2	Ranging and Location Statistics	66
7.3	The Multi-Path effect in the presence of the human body	66
7.4	Using 2 tags on right shoulder as best performance	67

Acronyms

RTLS

Real Time Locating System

IPS

Indoor Position Systems

GPS

Global Positioning System

WSN

Wireless Sensor Network

BLE

Bluetooth Low Energy

KF

Kalman Filter

EKF

Extended Kalman Filter

RF

RF Radio Frequency

RSS

Received Signal Strength

RSSI

Received Signal Strength Indication

AoA

Angle of Arrival

ToA

Time of Arrival

OW-ToA

One way Time of Arrival

TW-ToA

Two way Time of Arrival

UWB

Ultra Wide Band

SNR

Signal noise ratio

AWGN

additive white Gaussian noise

IoT

Internet of things

PV

Position velocity

Wi-Fi

Wireless Fidelity

Chapter 1

Introduction

1.1 Real-Time Locating System Applications

RTLS allow you to locate people or enterprise assets in real time. For deployment of a RTLS we use an ideal technology IPs which is base on WSN. A WSN is designed to locate, in specific places of the network, sensors able to read different types of data, depending on the type of system, such as temperature, motion, etc. RTL combines hardware and software to periodically provide the real-time position of a moving capable asset using mobile nodes, called “Tags”. These tags will communicate with fixed sensors with known position, estimated in coordinates, called “Anchors” [1]. This localization estimation of a real-time position is obtained in two phases of ranging and positioning. The first one estimates the distance between mobile and anchor nodes, while the second one uses these distance measurements to localize the mobile node in the system based on coordinates. There are several practical cases where having an IPS could be of great utility, such as smart structures to respond to earthquakes and make the buildings safer; precision agriculture by watering and fertilizing only where is necessary; maintenance exactly when and where is needed; traffic monitoring systems with better control stoplights and inform motorist for alternative routes; and environmental monitoring networks sensing air, water ,and soil quality and identifying the source of pollutants in real-time. There are two types of IPS systems which are Distributed and Centralized systems. In a distributed system the location of the mobile node is calculated by himself, this mobile node is cheap and with limited computation capabilities. In a centralized system, the locations of the mobile nodes are calculated by the control center connected to the central gateway. Today, thanks to advances in RF, it is possible the use of large networks of wireless sensors for monitoring and controlling applications. As is possible to see, there are a lot of useful applications and implementations in the market for indoor positioning, increasing the interest

for IPS, that is the motivation to develop it, taking advantage of the UWB systems due to its benefits. According to the above, it was proposed this thesis to develop an IPS based on a UWB technology that uses at TV studios.

1.2 Objective of Thesis

This thesis has several objectives to design and implement a 3D indoor localization algorithm suitable for real-time augmented reality applications to be applied in TV studios. In particular, the localization system has to accurately localize in parallel up to eight UWB wearable devices.

Indoor localization systems will be based on UWB technology.

The main goal is generating algorithms for 3D localization in indoor environments and then optimize and make robust these algorithms to mitigate the interference effect that the human body might cause to the UWB signal.

The performance of the overall system will be evaluated offline taking as input real measurements, provided by the LINKS personnel, collected in a real TV studio.

1.3 Overview of Thesis

After this introductory chapter, chapter 2 will explain an overview of Indoor Localization Systems as the most used ranging techniques. The two kind of approaches used in these systems and the localization algorithms where is specified the models used later in the implementation.

Chapter 3, provides an overview of the ranging measurements campaign for 3D Localization explaining its characteristics. Measurements have been performed in RAI TV studio, where eight UWB anchors and twenty-five test points are available. At the end of the chapter, distance measurement scenario is described and the best ranging performance evaluation for different cases without having obstacle and with human body are shown.

Chapter 4, discuss the evaluation of the 3D Localization Algorithm for 1 Tag. To meet this objective, an extended Kalman filter is used to evaluate the best performance for different models. At the end of this chapter, KF and EKF tracking algorithms have been analyzed in details. In addition, EKF is simulated to show its features and how its parameters change the tracking performance.

Chapter 5, represent the evaluation of 3D localization algorithm for 2 Tags by applying EKF and realizing the best performance for two models.

Chapter 6, present the evaluation of 3D localization algorithm for 3 Tags by using EKF and finding the best performance for two models.

In the last chapter, by comparing chapters 4, 5, and 6, the best performance model is evaluated and conclusions can be found.

Chapter 2

Overview of Indoor Localization systems

2.1 Introduction

RTLS are a combination of hardware and software used to establish and give real-time information about the location of assets and resources, such as objects, people, animals or anything equipped with devices designed to work with the system. GPS is the most pervasive example of an RTLS which is a well-known satellite-based technology that is used, assuming the availability of the appropriate hardware and software, to find a GPS-equipped device geographically worldwide. This is a truly noticeable system that has irrevocably convert the face of commercial and personal navigation. However, some problems appear when talking about indoors and the technology that GPS provides has strong limitations to work indoors.

As a result, the need to discover some technology appropriate for indoor location capability got increased. Basically, an indoor locating system is based on some localization hardware that is formed by a small number of sensors, called reference nodes, with fix known coordinates (either via GPS or from a system administrator during startup) and the unknown-location nodes or tags (facing the power supply problem that they have limited energy to work with). RTLS is based on many types of communication technologies, such as RF or optical systems (infrared), or acoustic (ultrasound). Future RTLS systems are predicted to be based on low power electronic tags used to follow and/or monitor assets, people, or anything of value with very high accuracy and mobility. Some example of radio frequency solutions are BLE, Zigbee, UWB and WIFI.

BLE is a low power wireless communication technology that can be used over a short distance to enable smart devices to communicate

Zigbee is a wireless technology developed as an open global standard to address the

unique needs of low-cost, low-power wireless IoT networks. The Zigbee standard operates on the IEEE 802.15.4 physical radio specification and operates in unlicensed bands including 2.4 GHz, 900 MHz and 868 MHz, as shown in Figure 2.1

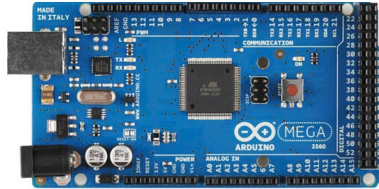


Figure 2.1: One example of Zigbee

UWB Like Bluetooth and Wi-Fi is a short-range, wireless communication protocol that operates through radio waves. Ultra-wide-band signals are well known procedures for high-bandwidth ToA estimations and is used for positioning applications because allows centimeter accuracy in ranging, as well as low power and low cost implementation of communications.

Nevertheless, there are two major disadvantages related to RTLS tags.

Firstly, the wide band based RF technology provide accurate localization solutions, while relatively narrow band based RF technology do not provide a sufficient level of accuracy required by applications.

Secondly, the RF technology can be large and power-hungry. This finding a trade off between accuracy and power consumption is the goal of RTLS design [5].

UWB is an attractive way to perform localization, especially for RTLS that require an accurate position information and high measurement rate. The UWB technology with ToA measurements, resulting in high accurate ranging estimates even in strong multi-path environments. Based on RF signals which spread over a large bandwidth, short pulses transmitted between UWB nodes are utilized for estimating the required travel time for the RF signal. Even though the ToA technique for UWB ranging provides accurate results, exact synchronization (usually through hardware) of the transmitting and receiving devices is a requirement. Through utilizing the coherent transmission capabilities of UWB signals and through implementing the TW-ToA technique, synchronization issues are resolved to a great extent. TW-ToA relies on the calculation of the time the RF signal requires for traveling from the transmitter to the receiver, the processing and transmission time at the receiver's part and the time for traveling back to the transmitter Figure 2.3. [11]

2.2 Ranging Techniques

To figure out the location of a tagged object, in 2D or 3D space, it is significant to determine and establish its distance from diverse well-known points. Through

learning and doing some generally basic calculations it is feasible to figure the position of the tag. There are various techniques for implementing ranging utilizing wireless schemes. These are divided basically into three types of schemes. First, Radio Signal Strength-based, normally referred to as Received Signal Strength Indication or RSSI schemes, second AoA and third ToA. In this thesis, the main focus is on ToA.

2.2.1 RSSI

RSS is the power of received signal estimated by a receiver's RSSI circuit. Frequently, RSS is reported as estimated power, i.e., the squared magnitude of the voltage. Wireless sensors connect to neighboring sensors, so every beneficiary amongst ordinary information communication without introducing extra bandwidth or energy requirements can estimate the RSS of RF signs. RSS assessments are generally easy to execute in hardware equipment. However, RSS estimations are unstable and the driving distance estimation is inaccurate.

2.2.2 OW-ToA

The main idea supporting ToA method is that the distance between the sender and the receiver of a signal can be obtained by measuring the signal propagation time and the signal's known velocity. Two ways for the calculation ToA are OW-ToA and TW-ToA. In one-way, the difference between the send and arrival of the signal is calculated using high precision synchronization of the clocks of the sender and receiver. For one-way measurements, the distance between two nodes i, j can be calculated as

$$dist = (t_2 - t_1)V \tag{2.1}$$

Where t_1 and t_2 are the send and receive time of arrival of the signal measured at the sender and receiver respectively, as Shown in Figure 2.2 [4]

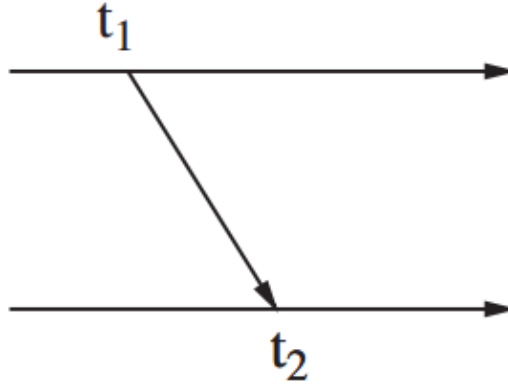


Figure 2.2: Temporal diagram for one way ToA

2.2.3 TW-ToA

In two-way method the round trip of the signal is measured at the sender node and t_3 and t_4 are the send and receive times of the response signal.

$$dist = \frac{(t_4 - t_1) - (t_3 - t_2)}{2}V \quad (2.2)$$

We can observe that with the one-way approach the receiver node calculates its position while in two-way method the sender calculates the distance to the receiver and must then report the location using an extra message, as shown in Figure 2.3 Advantage of this technique is more robust to the multi-path channel than the RSS technique by assuming that there is a direct path between transmitter and receiver. The difficulty of implementing a time based technique is the receiver's ability to accurately estimate the arrival time of the LoS signal hampered by additive noise and multi-path signals.

The best achievable accuracy of ToA based distance estimate under single path additive white Gaussian noise (AWGN) channel satisfies the following inequality [10]

$$\frac{c}{2\sqrt{2}\sqrt{SNR}\beta} < \sqrt{var(d - \hat{d})} \quad (2.3)$$

Where \hat{d} is the estimated distance between two nodes while d is the corresponding exact distance. c is the speed of light and β is the effective bandwidth of the transmission signal. Hence, the ToA ranging accuracy is improved by increasing the SNR or the effective signal bandwidth. This is the main reason why UWB technology is widely used in time-based ranging method.

Errors in ToA estimation are caused early arriving multi-path, when many multi-path signals arrive very soon after the LoS signal and their contributions to the

cross correlation obscure the location of the peak from the LoS signal. The second cause of error is the attenuated LoS that can be severely attenuated compared to the late arriving multi-path components, causing it to be lost in the noise and missed completely. The attenuated LoS problem, is only severe in networks with large inter sensor distances so using a cooperative localization approach avoids large errors also in these kind of networks. Early arriving multi-path components cause smaller errors but are very difficult to combat.

Generally, wider signal bandwidths are necessary to obtain greater temporal resolution. The peak width of the auto-correlation function is inversely proportional to the signal bandwidth. A narrow auto-correlation peak enhances the ability to identify the arrival time of a signal and helps in separating the LoS signal cross correlation contribution from the contributions of the early arriving multi-path signal justifying the use of UWB signals to calculate the ToA in localization systems. [11]

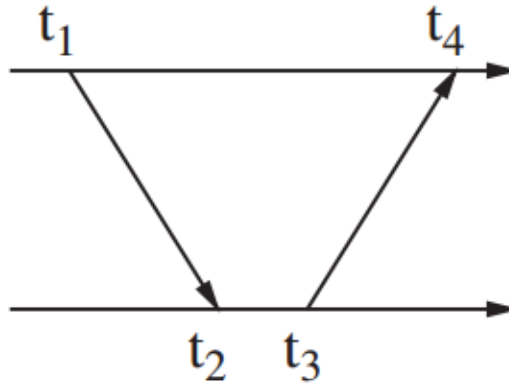


Figure 2.3: Temporal diagram for two way ToA

2.3 Localization Algorithms

There are two main stages to estimate the position when working with wireless positioning systems. A ranging technique is utilized in the initial stage, as ToA or RSS the most widely used, to measure the distance between the tag and the anchors, at that point in the second stage, this data is applied as a part of the location algorithms to estimate the tag's position. KF and EKF are Bayesian methods that can be applied for indoor localization.

The Bayesian positioning approach considers the probability and statistics of these measurements and the a priori mobile's positions. The Bayesian tracking approach models the tracking problem as a discrete time stochastic process.

2.3.1 KF

Rudolph Kalman introduced The Kalman Filters (KF from now on) back in and 1960. Since then, they have been extensively used in both applied science and economics. They are elegant and efficient algorithms for localization, Due to its statistical treatment, at least while both the system and measurements behave linearly and normally distributed. However, these conditions are not always satisfied, the reason why some linearization and approximations are performed expanding the applications of the KF in the form of the EKF.

2.3.2 EKF

The Kalman Filter algorithm, provides a satisfactory, effective and practical solution for location issues when the system is linear, and measurement errors are modelled according to Gaussian distribution. Since these conditions do not generally occur, some linearization and approximations are expected to exchange the KF into the EKF, appropriate for non-linear systems [6]. The discrete EKF modeled by discrete-time state equation can measure recursively the condition of a dynamic system.

$$\mathbf{x}_k = f(\mathbf{x}_{k-1}) + w_k \quad (2.4)$$

$$w_k = \mathcal{N}(0, \mathbf{Q}_k) \quad (2.5)$$

Where \mathbf{x}_k the state vector at time k, f is the state transition function which evolves the state in time given the previous state. The random process noise vector w_k takes into account the non linearity and perturbations of the system normally distributed with zero mean and co-variance matrix Q_k . The system is observed through the following measurement equations[7]

$$z_k = h(\mathbf{x}_k) + \mathbf{v}(k) \quad (2.6)$$

$$\mathbf{v}_k = \mathcal{N}(0, \mathbf{R}_k) \quad (2.7)$$

Where z_k the measurements vector at time k, h_k is the observation function which estimates the expected measurements at the state \mathbf{x}_k and v_k is the random observation noise vector assumed normally distributed with zero mean and co-variance matrix R_k . The EKF is developed in two phases the predict phase and the update phase. The predict phase takes the previous state and does a predicted state with the system information and the update phase updates the estimate with the prediction correcting the error vector where finally in the same conditions the system will arrive to steady state.

$$\mathbf{x}_k = f(\mathbf{x}_{k-1}, u_{k-1}) + q_k \quad (2.8)$$

$$P_k = F_k P_{k-1} F_k^T + Q_k \quad (2.9)$$

Where q_k is the mean vector and Q_k the co-variance matrix of the system state noise vector w which is Gaussian distributed; and F_k is the Jacobian of the system transition function f calculated around the previous a posteriori state estimate \mathbf{x}_k . After finding these a priori values, the algorithm proceeds to the Measurement Update, correcting the estimates finding a weight factor for the measures according to their co-variance matrix and the state estimated.

$$S_k = \mathbf{H}_k P_k^- \mathbf{H}_k^T + \mathbf{R}_k \quad (2.10)$$

$$K_k = P_k^- \mathbf{H}_k^T S_k^{-1} \quad (2.11)$$

$$s_k = z_k - h(\mathbf{x}_k^-) \quad (2.12)$$

$$\mathbf{x}_k^+ = \mathbf{x}_k^- + K_k s_k \quad (2.13)$$

$$P_k^+ = (I_k - K_k P_k^-) P_k^- \quad (2.14)$$

s_k is the innovation vector and S_k its co variance matrix, K_k is the Kalman gain, R_k the co-variance of the Gaussian distributed measurement noise vector v_k . Like in the first step, H_k is the Jacobian around the a priori state estimate \mathbf{x}_k of the observation function h . Both steps, just the first order derivatives are used for the Jacobian, and accuracy can be improved with higher order Jacobian. The performance of the Kalman Filter in general depends on how well the systems are modeled and the initial parameters chosen, so a survey of some models inside the scope of this research are presented on next.

Chapter 3

Ranging Measurements Campaign for 3D Localization

3.1 Introduction

A measurement campaign has been carry out in RAI by using UWB devices from synchronicIT. This measurement were done in different scenarios without obstacle and with human body. For without obstacle the measurements are base on two different tripod 93 cm and 153 cm and with human body three measurements which consist of right shoulder 156 cm, right pocket 77 cm and back belt 93 cm are considered. By calculating ranging error the best performance for scenario of without obstacle and with human body will be observed.

3.2 Deployment of the UWB Localisation System

This thesis was meant to be designed and implemented an RTLS based on the UWB. The UWB-based Localization System has been deployed in an indoor area by the Anchors, as shown in Figure 3.2 and the Tags shown in Figure 3.1.

They will be exchanging ranging messages between them to let the tags estimate their position based on a coordinate system. In this thesis, the number of test points is twenty-five and the Localization system will be based on indoor area in which 8 anchors were disposed to range with up to three tags that are programmed to work, as shown in Figure 3.3



Figure 3.1: Tag - size 4.6 x 7.3 cm



Figure 3.2: Anchor - size 9.8 x 9.8 cm

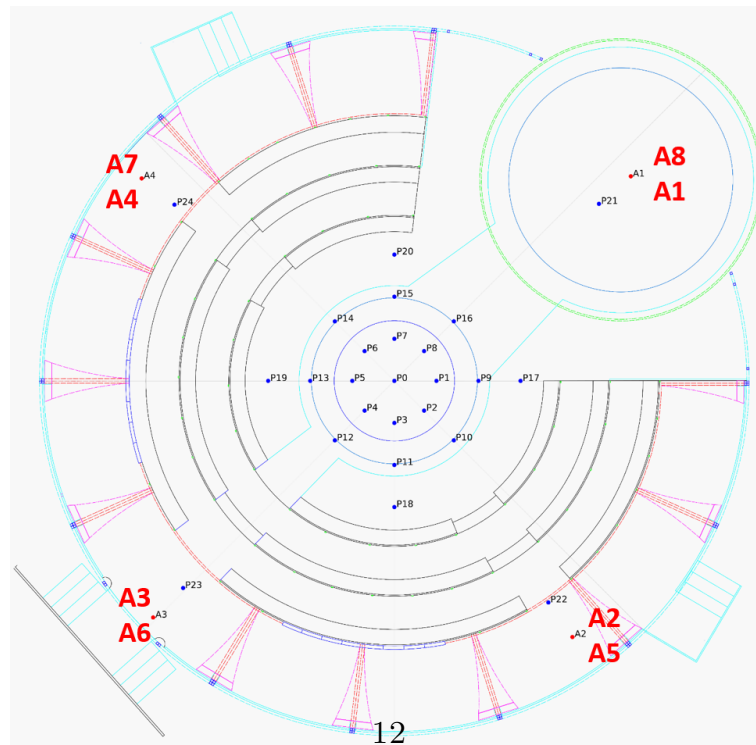


Figure 3.3: Test points

3.3 Distance Measurement Scenarios

In this thesis two measurement scenarios are considered. Firstly, measurements in static condition and secondly, measurements in dynamic condition. Ranging measurement have been performed without obstacles deploying the tag on tripod at two different height 93 cm and 153 cm, as shown in Figure 3.4. In order to test interface of human body several tests have been done with the tag in right pocket, as shown in Figure 3.6, for tag on the back belt, as shown in Figure 3.5 and for tag on the right shoulder, as shown in Figure 3.7.

Some measurements have been done in dynamic condition by walking with a tag inside the right pocket, walking with a tag on the back, walking with a tag on the right shoulder, running with a tag inside the right pocket, running with a tag on the back and running with a tag on the right shoulder.



Figure 3.4: Tripod - height 93 cm and height 153 cm



Figure 3.5: Back belt - height 93 cm



Figure 3.6: Right pocket - height 77 cm



Figure 3.7: Right shoulder - height 156 cm

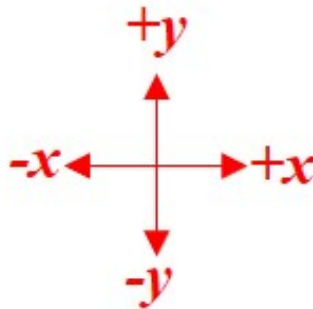


Figure 3.8: 4 orientation of Human body Ranging Localization

For ranging with human body four orientation $+x$, $+y$, $-x$ and $-y$ for different test points have been considered, as shown in Figure 3.8

3.4 Ranging Performance Evaluation

For evaluating ranging error, calculation of ranging error of average μ^i , average standard deviation σ^{ij} and RMS^i are done by using the following formula

$$\mu^i = \frac{1}{N} \sum \epsilon_k^i \quad (3.1)$$

$$\sigma^{ij} = \sqrt{\frac{1}{N-1} \sum (\epsilon_k^i - \mu^i)(\epsilon_k^j - \mu^j)} \quad (3.2)$$

$$RMS^i = \sqrt{(\sigma^{ij})^2 + (\mu^i)^2} \quad (3.3)$$

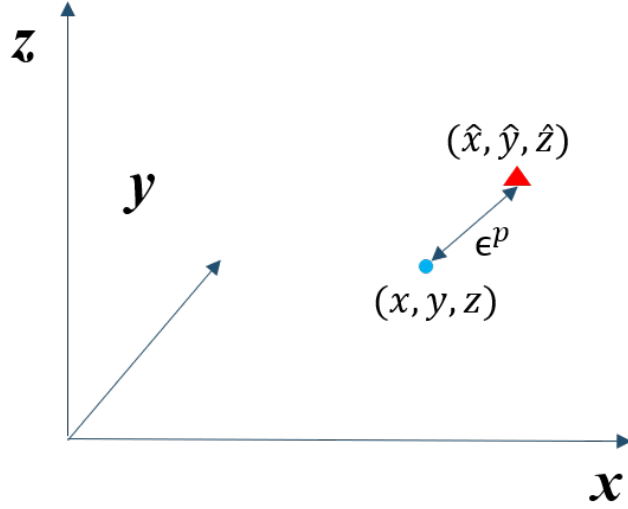


Figure 3.9: Error along the axes

As shown in Figure 3.9, error along x, y, z axes for position estimation of tags and for exact location of them can be evaluated by formula 3.4, 3.5 and 3.6.

$$\epsilon^x = \hat{x}_i - x_i \quad (3.4)$$

$$\epsilon^y = \hat{y}_i - y_i \quad (3.5)$$

$$\epsilon^z = \hat{z}_i - z_i \quad (3.6)$$



Figure 3.10: Static Ranging Localization

For static ranging localization, first for ranging distance measurement and exact distances are evaluated, as shown in Figure 3.10

Then error for distance can be calculated by having value of distance measurement and exact distances, as shown in formula 3.7

$$\epsilon^d = \hat{d}_i - d_i \quad (3.7)$$

For localization, evaluation for position estimation of tags and exact location of them have been calculated, as shown in Figure 3.10 and then by using Formula 3.5, error of 3D position and by using Formula 3.6 error of 2D position can be evaluated.

$$\epsilon_k^p = \sqrt{(\hat{x}_k - x_k)^2 + (\hat{y}_k - y_k)^2} \quad (3.8)$$

$$\epsilon_k^p = \sqrt{(\hat{x}_k - x_k)^2 + (\hat{y}_k - y_k)^2 + (\hat{z}_k - z_k)^2} \quad (3.9)$$

3.4.1 Without Obstacle

3.4.1.1 Measurements in static condition

For this case, two different tripod are considered. First with 93 cm height and then tripod with 153 cm height. Test point 0 is one example of the 25 test points and performance of 8 anchors for this specific test point is shown in Figure 3.11 and Figure 3.12.

Anchor 3 has less number of errors among 8 anchors and there is no evaluation for anchor 5, as shown in figure 3.12

Ranging Measurements Campaign for 3D Localization

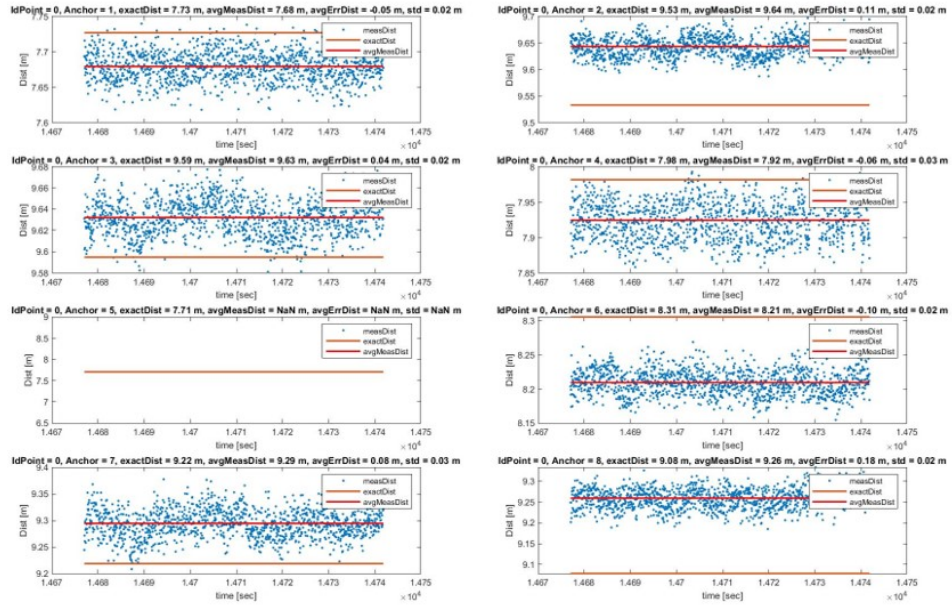


Figure 3.11: Ranging without obstacles ($h = 93$ cm), (Test Point 0)

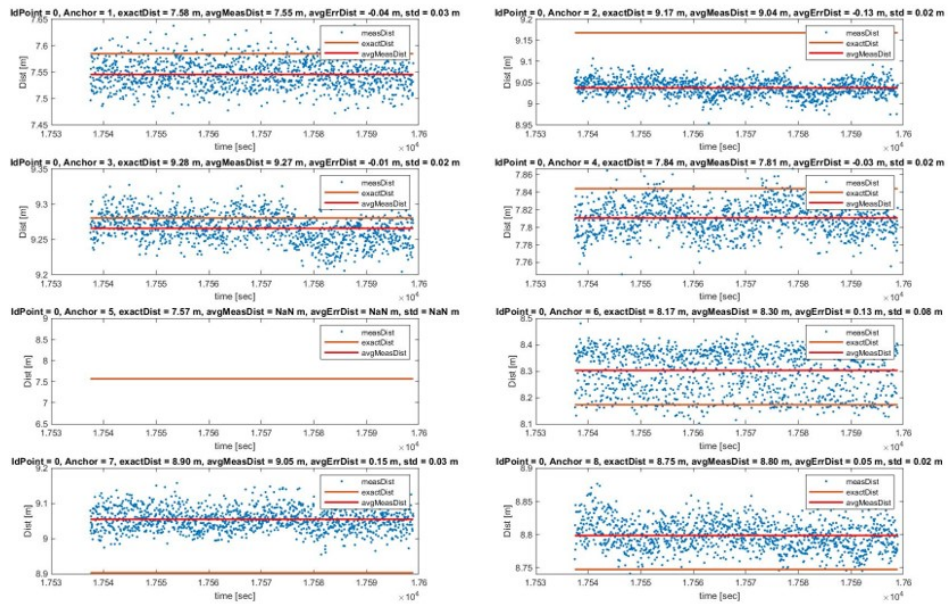


Figure 3.12: Ranging without obstacles ($h = 153$ cm), (Test Point 0)

Table 3.1 shows global performance and average error for tripod with 93cm and 153cm height. Tripod with height 153cm has smaller number of errors comparing with tripod with 93cm height. As result, tripod 153cm height has the best performance. Multi-Path effect occasionally happens when the distance is estimated not on the direct radius but on the reflected path, introducing an error on the measurement, as shown in Figure 3.13.

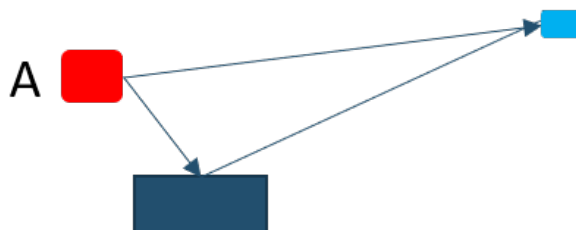


Figure 3.13: Multi-Path Effect

Static Tag on Tripod with height = 93 cm
avdErrDist = 0.02 m
stdErrDist = 0.21 m
Static Tag on Tripod with height = 153 cm
avdErrDist = 0.003 m
stdErrDist = 0.14 m

Table 3.1: Global statistics for ranging with Tripod

3.4.2 With Human body

3.4.2.1 Measurements in static condition

Five different test points 0,12,16,21,23 in four orientations were checked. As example test point 21 with orientation +y when the tag is on right shoulder is shown in Figure 3.14, test point 21 with orientation -y, when tag is on back belt is shown in Figure 3.15 and test point 21 with orientation +y when tag is on right pocket is shown in Figure 3.16.

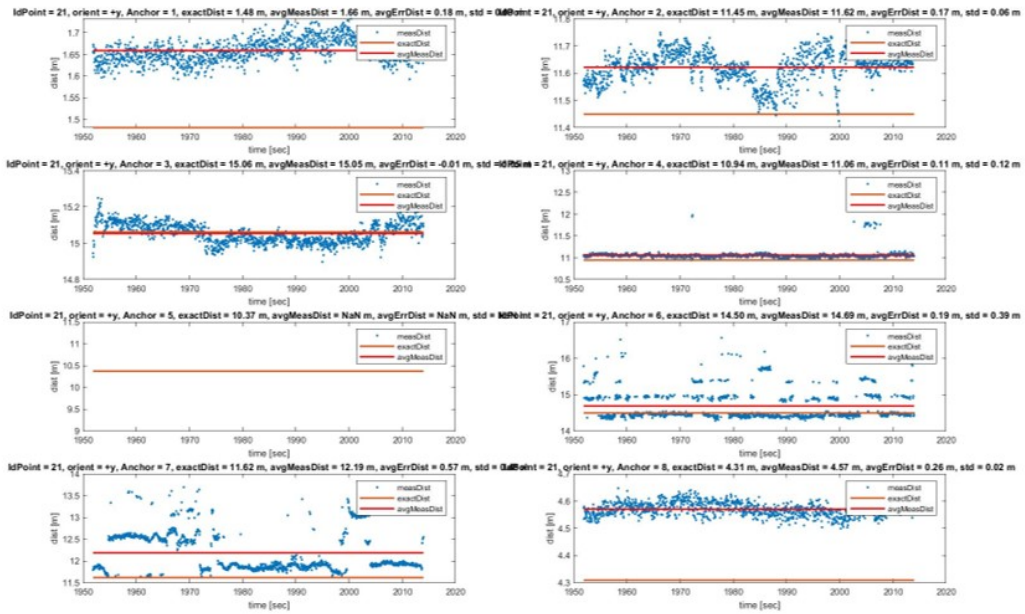


Figure 3.14: Ranging with right shoulder ($h=156$ cm), (Test Point 0)

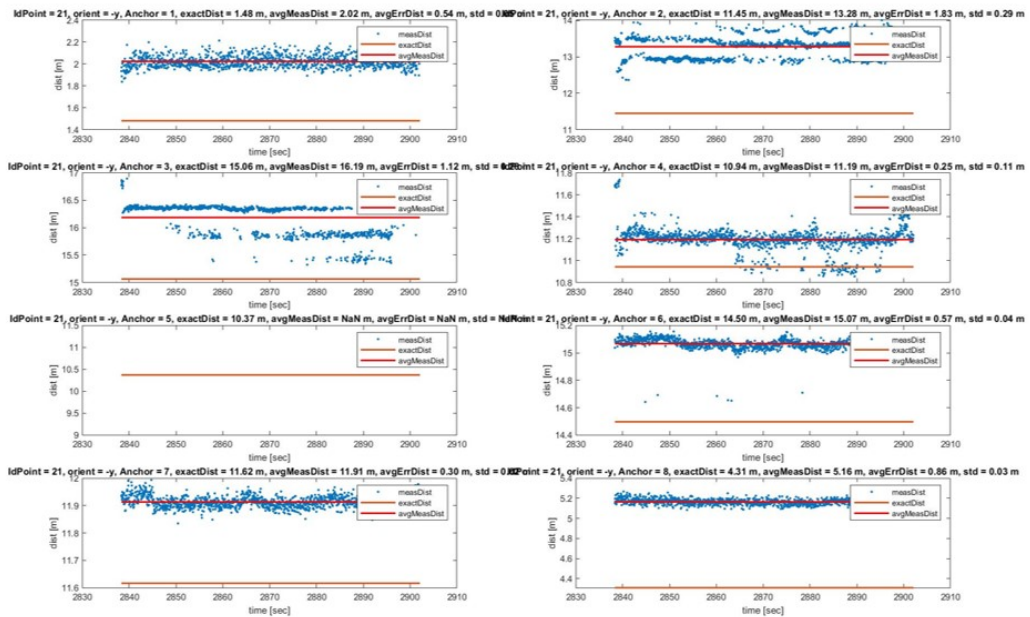


Figure 3.15: Ranging with Human body (tag on the back belt $h = 111$ cm)

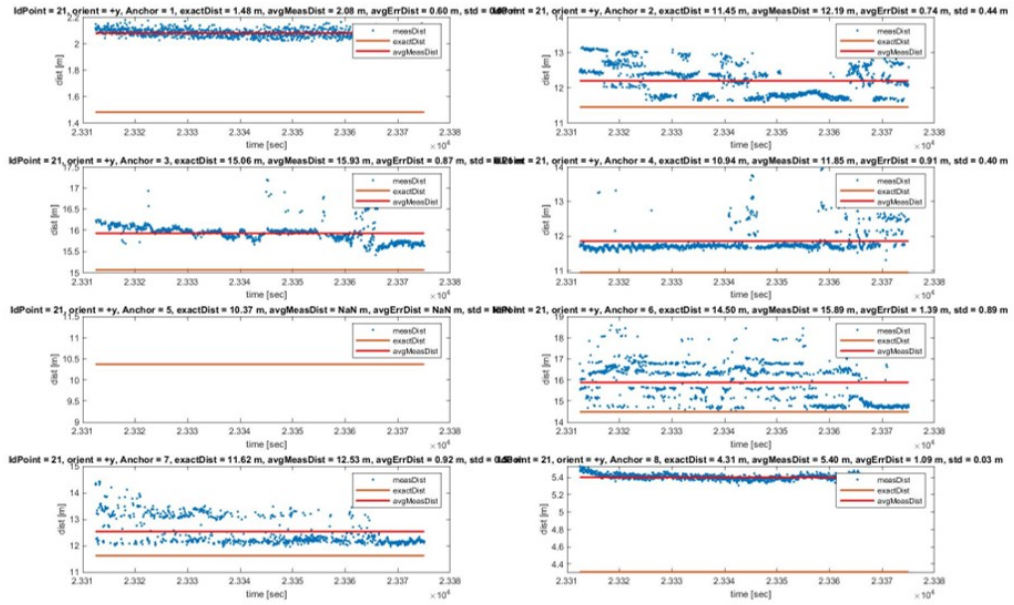


Figure 3.16: Ranging with Human body (tag inside the right pocket $h = 77 \text{ cm}$)

Statistics global performance about ranging with tags on human body, are shown in table 3.2. First of all, Tag on the right shoulder has fewer errors and the most connectivity. The second best choice is tag behind the back on the belt which has better connectivity and the worse connectivity by having a lot of errors is for tag inside the right pocket.

Tag inside the right pocket
avdErrDist = 0.45 m
stdErrDist = 0.66 m
Connectivity = $7 / (20 * 7) = 5.0$ percent
Tag behind the back on the belt
avdErrDist = 0.28 m
stdErrDist = 0.50 m
Connectivity = $(20 * 7 - 16) / (20 * 7) = 88.6$ percent
Tag on the right shoulder
avdErrDist = 0.12 m
stdErrDist = 0.62 m
Connectivity = $(20 * 7 - 6) / (20 * 7) = 95.7$ percent

Table 3.2: Global statistics for ranging with Human body

The Multi-Path effect in the presence of the human body is more pronounced and distance is estimated not on the direct path but on the reflected path. The tag on the right shoulder shows the best performance for human body shown in Figure 3.17

In general, the Multi-Path effect in the presence of the human body is more pronounced than in the case with tags on a tripod the localization error on the shoulder is lower (less subject to multi-path). In fact, the error on ranging measurements is lower than tag on back belt and right pocket, As shown in Table 3.2.

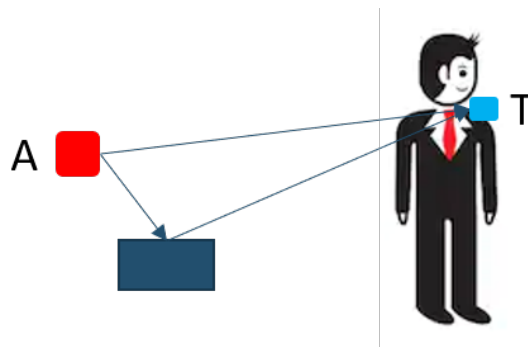


Figure 3.17: The Multi-Path effect in the presence of the Human body

Chapter 4

Design and Evaluation of the 3D Localization Algorithm - 1 Tag

4.1 Design of the EKF for 3D Localization for 1 Tag

In this chapter, the EKF algorithm for 1 tag was simulated and tested in Matlab. First of all, observation has been done for tag on 153 cm tripod as the best model without obstacle which has been chosen in previous chapter.

Second, the evaluation of tag on right shoulder as the best model with smaller number of errors with human body was evaluated.

For this purpose, for designing EKF for 1 tag, the simulation has been done for two state models, P and PV model (which in this chapter these two models will be introduced later). As a result, the best σ_a for these state models has been chosen and the best performance without obstacle and with human body are evaluated.

4.1.1 State Models

The first step to design a good EKF is to formulate a state model that describes the system dynamics. In particular, this research is interested in improving the localization accuracy on applications with statics and dynamics (walk or run) while keeping a systems that is implementable in different scenarios, so two basic models are studied. The models here presented are developed in 3D space and $n = 1, 2, 3$ is an indicator of the space dimension.

4.1.2.1 P model

This model can be viewed as a static version of the EKF, in other words it just performs the measurement update. Generally has two applications, one is to filter and estimate some measurement parameters knowing the exact position and the second one is tracking, where due to low sampling frequencies for instance, a dynamic model does not work well and a priori positions are predicted as random variables inside a certain region (described by the process noise co-variance matrix). This matrix has a great impact on the EKF performance, with lower values a smooth output will be obtained but with larger settling times, so a variable Q_k is presented as function of the time transurred between two measures Δ_T and the standard deviation σ_a of a Gaussian distributed acceleration vector and $I_{3,3}$ is 3x3 identity matrix. The state equation would be

$$\mathbf{x} = [x, y, z]^T \quad (4.1)$$

$$\mathbf{x}_k = f(\mathbf{x}_{k-1}, 0) = I_{3,3}\mathbf{x}_{k-1} \quad (4.2)$$

$$\mathbf{Q}_k = [\Delta_T I_{3,3}] [\Delta_T I_{3,3}]^T \sigma_a^2 \quad (4.3)$$

4.1.2.2 PV model

It is a dynamic EKF and assumes near constant velocity between the estimation intervals Δ_T . Again the process noise is a key factor, and smooth tracking will be gotten if we consider zero or small white accelerations. However on non-linear maneuvers (velocity is not longer constant) slow response or even divergence will be appreciated, anyway if process noise is set large enough, some of these maneuvers can be tracked with noisier tracking. Its state vector is expressed as

$$\mathbf{x} = [x, y, z, v_x, v_y, v_z]^T \quad (4.4)$$

$$\mathbf{x}_k = F(\mathbf{x}_{k-1}, 0) = \begin{bmatrix} I_{3,3} & \Delta_T I_{3,3} \\ O_{3,3} & I_{3,3} \end{bmatrix} \mathbf{x}_{k-1} \quad (4.5)$$

$$\mathbf{Q}_k = \begin{bmatrix} 1/2\Delta_T^2 I_{3,3} \\ \Delta_T I_{3,3} \end{bmatrix} \begin{bmatrix} 1/2\Delta_T^2 I_{3,3} \\ \Delta_T I_{3,3} \end{bmatrix}^T \sigma_a^2 \quad (4.6)$$

Δ_T is the elapsed time from previous time k to current time $k + 1$ and $I_{3,3}$, $O_{3,3}$ are 3x3 identity matrix and zero matrix, respectively. PV model is feasible in low acceleration movement scenario, that is, constant speed circumstance. There is a time interval during which the tracking algorithm estimates the speed, named

as transient stage. Moreover, we only care about the position of the tag and the measurements are only related to positions[12].

The process noise is modeled as independent random acceleration k normally distributed with zero mean and co-variance matrix \mathbf{Q}_k that allow the track of the different forces that could temporally affect target's dynamics [13].

where σ_a^2 is the variance random acceleration component of the process noise. This value is set manually according to the system and is a key factor in the EKF design zero or small variance random acceleration generally lead to a smooth tracking.

4.1.2 Measurement model

Most of tracking systems are based on some sort of distance estimates, we have N number of distance measurements While these estimates keep a Gaussian distribution, as shown in formula 4.7. The transformation between distances and coordinates is non-linear, and some linearizations has to be performed to compute the H_k matrix for P model and PV model. For calculating H_k we use \hat{d} which is the Euclidean distance evaluated at a priori estimation of the position as define in equation 4.8

H_k for P model is a matrix of $N \times 3$ as shown in formula 4.9 and PV model is a matrix of $N \times 6$ that consist of $O_{1,3}$ which is a zero matrix, as shown in formula 4.10.

$$\mathbf{z}_k = [z_{1,k}, z_{2,k}, z_{3,k}, \dots, z_{N,k}]^T \quad (4.7)$$

$$h(\mathbf{x}_k) = \begin{bmatrix} \sqrt{(x_k - x_{A_1})^2 + (y_k - y_{A_1})^2 + (z_k - z_{A_1})^2} \\ \sqrt{(x_k - x_{A_2})^2 + (y_k - y_{A_2})^2 + (z_k - z_{A_2})^2} \\ \vdots \\ \sqrt{(x_k - x_{A_N})^2 + (y_k - y_{A_N})^2 + (z_k - z_{A_N})^2} \end{bmatrix} \quad (4.8)$$

$$\mathbf{H}_k = \begin{bmatrix} \frac{x_k - x_{A_1}}{\hat{d}_{1,k}} & \frac{y_k - y_{A_1}}{\hat{d}_{1,k}} & \frac{z_k - z_{A_1}}{\hat{d}_{1,k}} \\ \frac{x_k - x_{A_2}}{\hat{d}_{2,k}} & \frac{y_k - y_{A_2}}{\hat{d}_{2,k}} & \frac{z_k - z_{A_2}}{\hat{d}_{2,k}} \\ \vdots & \vdots & \vdots \\ \frac{x_k - x_{A_N}}{\hat{d}_{N,k}} & \frac{y_k - y_{A_N}}{\hat{d}_{N,k}} & \frac{z_k - z_{A_N}}{\hat{d}_{N,k}} \end{bmatrix} \quad (4.9)$$

$$\mathbf{H}_k = \begin{bmatrix} \frac{x_k - x_{A1}}{\hat{d}_{1,k}} & \frac{y_k - y_{A1}}{\hat{d}_{1,k}} & \frac{z_k - z_{A1}}{\hat{d}_{1,k}} & O_{1,3} \\ \frac{x_k - x_{A2}}{\hat{d}_{2,k}} & \frac{y_k - y_{A2}}{\hat{d}_{2,k}} & \frac{z_k - z_{A2}}{\hat{d}_{2,k}} & O_{1,3} \\ \vdots & & & \\ \frac{x_k - x_{A_N}}{\hat{d}_{N,k}} & \frac{y_k - y_{A_N}}{\hat{d}_{N,k}} & \frac{z_k - z_{A_N}}{\hat{d}_{N,k}} & O_{1,3} \end{bmatrix} \quad (4.10)$$

The priori estimate is corrected using all the distance measurements available at each step, but this requires to have (or at least assume) simultaneous measurements, which is not always feasible. Another issue is the linearized H_k matrix, iterations around a posteriori estimates can improve accuracy (not always true), but if the a priori estimate is good, no significant improvement is noticed.

4.2 Evaluation of Localization Performance and Optimization

The evaluation has been done in two different conditions. First in static condition without obstacle and second in static condition with human body.

For condition without obstacle, tripod with 153 cm for two different models of P model and PV model and For condition with human body, by using 1 tag on right shoulder and generating EKF for 1 Tag, the best performance of σ_a as one parameter of Q_k matrix are evaluated. (right shoulder comparing with two other models has best performance and smaller number of errors. For this reason, only this scenario is mentioned in this chapter).

At the end, after evaluating static condition for human body, evaluation for dynamic condition for three different scenarios right shoulder, right pocket and back belt are evaluated.

4.2.1 Static Condition without Obstacles

First, by using EKF algorithm, Localization performance for test Point P0 for ranging measurements without obstacles with height of the tripod 153 cm is considered and then by optimizing σ_a which is one of parameters of Q_k matrix, the best σ_a for our localization system is selected.

4.2.1.1 P model

For evaluating different value of σ_a as one parameter of Q_k matrix for P model in our EKF algorithm, first different test points (Test point 0 is one example of

test points that was evaluated, as shown in Figure 4.1), different value of rmse for each σ_a were obtained, as shown in Figure 4.2. The best performance for static condition without obstacle in case of P model is when $\sigma_a = 5$, as shown in Figure 4.3

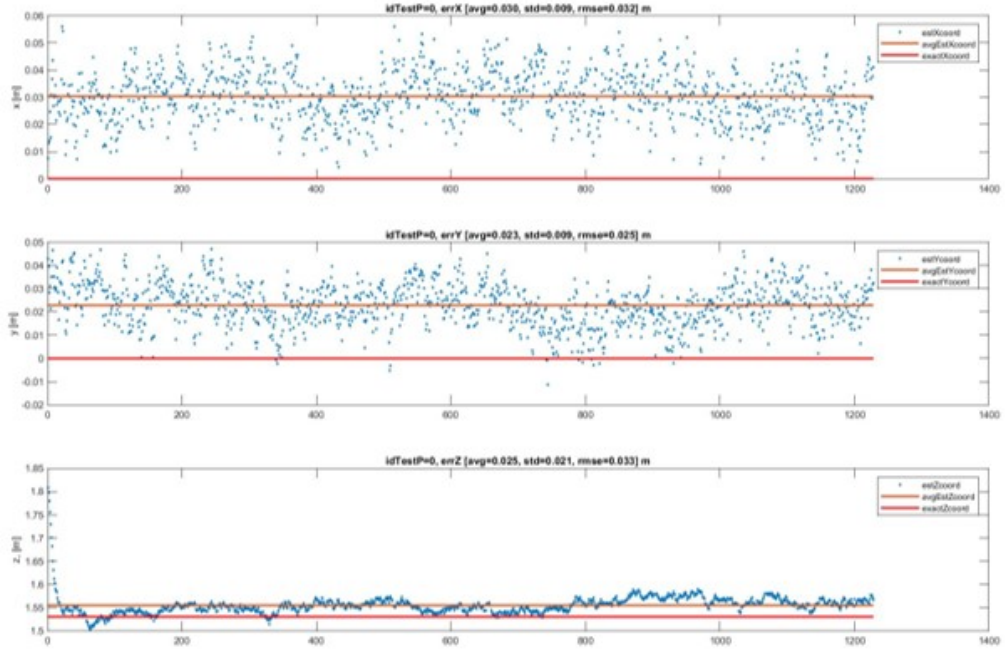


Figure 4.1: Test point 0 - 3DLocErr [avg=0.049, std=0.017, RMS=0.052]m

Performance	
2DLocErr	[avg=0.060, std=0.050, RMS=0.078] m
3DLocErr	[avg=0.110, std=0.114, RMS=0.158] m
XErr	[avg=-0.012, std=0.053, RMS=0.054] m
YErr	[avg=-0.005, std=0.056, RMS=0.057] m
ZErr	[avg=-0.045, std=0.130, RMS=0.138] m

Table 4.1: Performance of $\sigma_a=5$ for P model

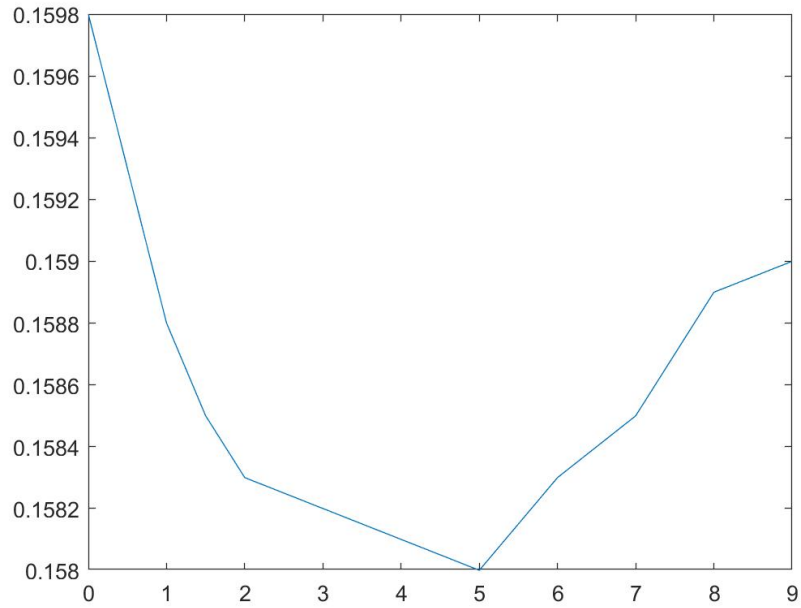


Figure 4.2: Ratio between σ_a and rmse as a function of σ_a

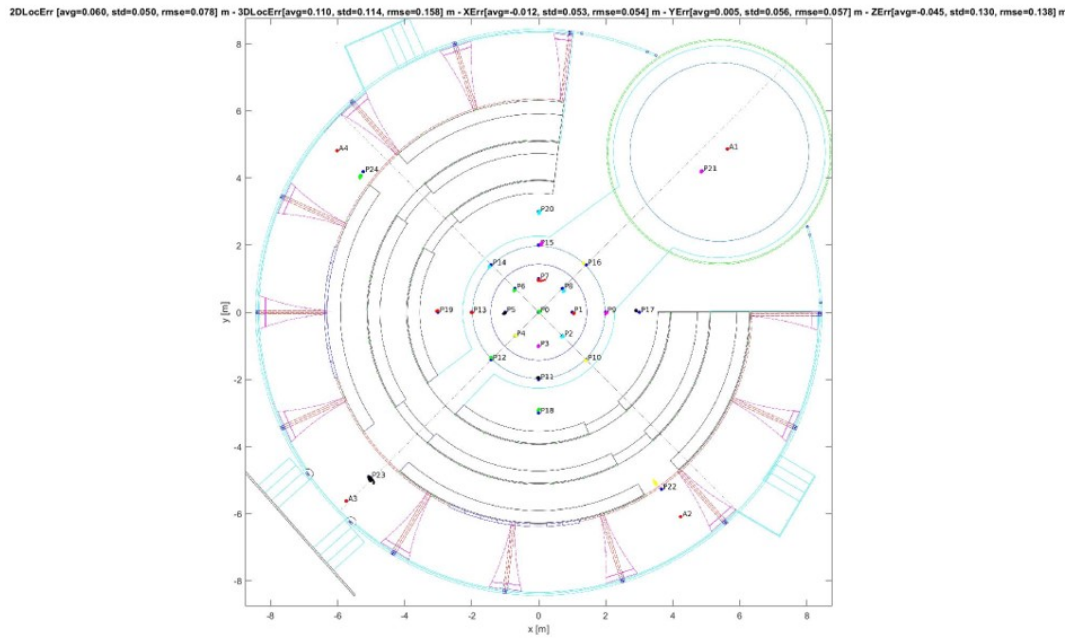


Figure 4.3: P model for 1 Tag - without obstacle (153cm)

When $\sigma_a = 5$ the errors for 2D localization and 3D localization are 0.078 and 0.158, as shown in Figure 4.3 and Table 4.1.

4.2.1.2 PV model

σ_a is one parameter of Q_k matrix for different test-points (Figure 4.4 is one example of test-point 0 that shows error for 3 different axes x, y, z). In our EKF algorithm for 1 Tag, experiment has been done by having different value for σ_a , so as result each σ_a has specific value of rmse, as shown in Figure 4.5. The best performance for static condition without obstacle in case of PV model is when $\sigma_a = 6$, as shown in Figure 4.6 and table 4.2

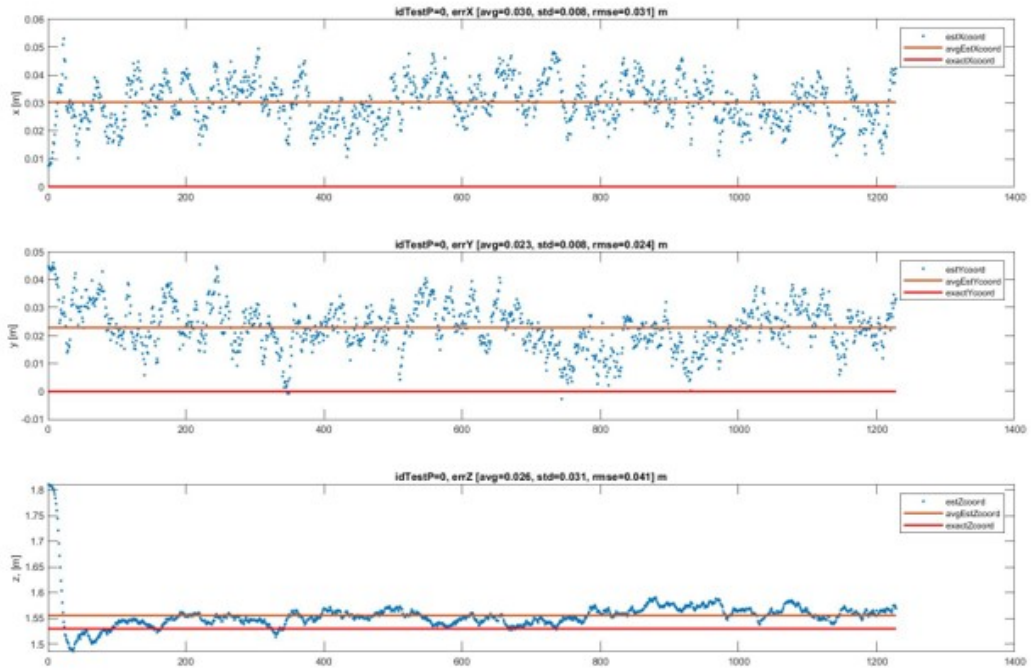


Figure 4.4: Test point 0 - 3DLocErr [avg=0.050, std=0.026, RMS=0.057] m

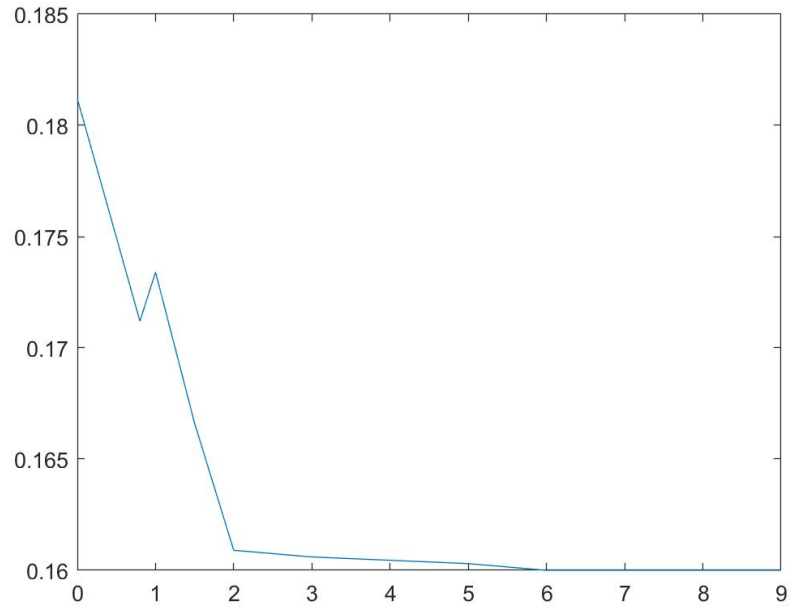


Figure 4.5: Ratio between σ_a and rmse as a function of σ_a

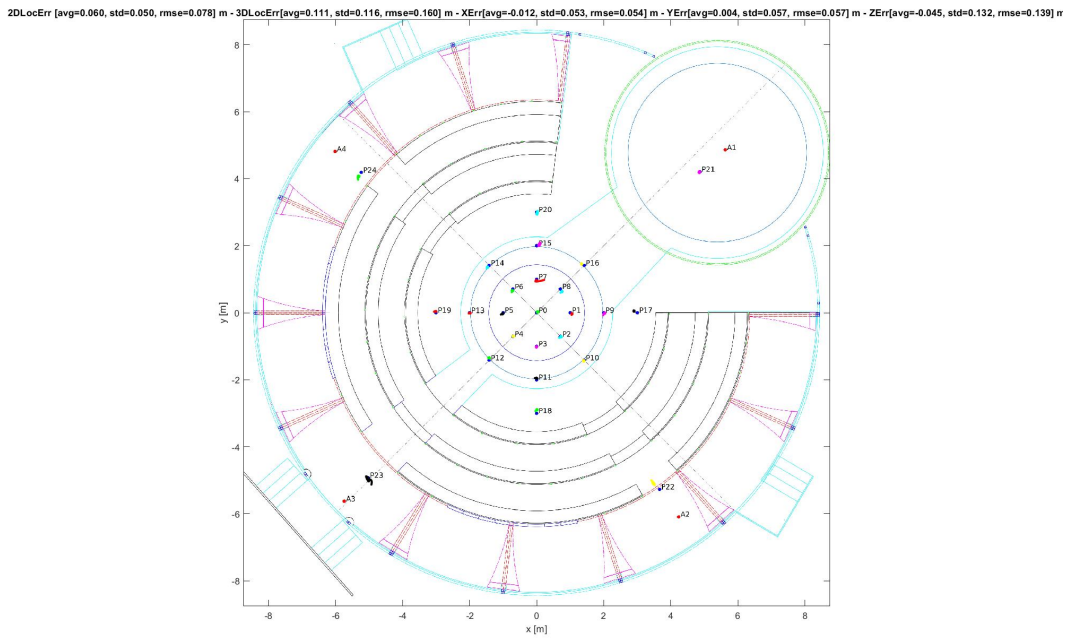


Figure 4.6: Global error of PV model for 1 tag - without obstacle(153 cm)

Performance	
2DLocErr	[avg=0.060, std=0.050, RMS=0.078] m
3DLocErr	[avg=0.111, std=0.116, RMS=0.160] m
XErr	[avg=-0.012, std=0.053, RMS=0.054] m
YErr	[avg=-0.004, std=0.057, RMS=0.057] m
ZErr	[avg=-0.045, std=0.132, RMS=0.139] m

Table 4.2: Performance of $\sigma_a = 5$ for PV model

Error for 3D localization and 2D localization for tripod with 153 cm height is less than tripod with 93 cm height (as shown in previous chapter tripod 153 cm has smaller number of errors). As far as the choice of σ_a (one parameter of Q_k matrix in EKF algorithm) affects the localization performance. So, $\sigma_a = 5$ with rmse = 0.158 for P model have been chosen as the best performance when there is no obstacles.

4.2.2 Static Condition with Human Body – 1 Tag on the right shoulder

4.2.2.1 P model

In this model, by looking at Figure 4.7, test-point 0 for P model and the errors for three different axes x, y, z are shown. After that, by evaluating different value of σ_a as one parameter of Q_k matrix in our EKF algorithm for 1 Tag, different values of rmse will be obtained. The best performance that minimize the localization error for tag on right shoulder is when $\sigma_a = 0.01$, as shown in Figure 4.8.

4.2.2.2 PV model

Figure 4.9 is shown performance of test-Point P0 when tag is on right shoulder for PV model. By using EKF algorithm, the result shows that errors for this model are more than P model.

For PV model, after $\sigma_1 = 2$, for all value bigger that 2, errors were increased. $\sigma_a = 1$, $\sigma_a = 1.5$ and $\sigma_a = 2$ have the lowest number of errors and errors are same for all of them, as shown in Figure 4.10. So as result, we have smaller number of errors and the best performance when σ_a is any of these values 1, 1.5 or 2.

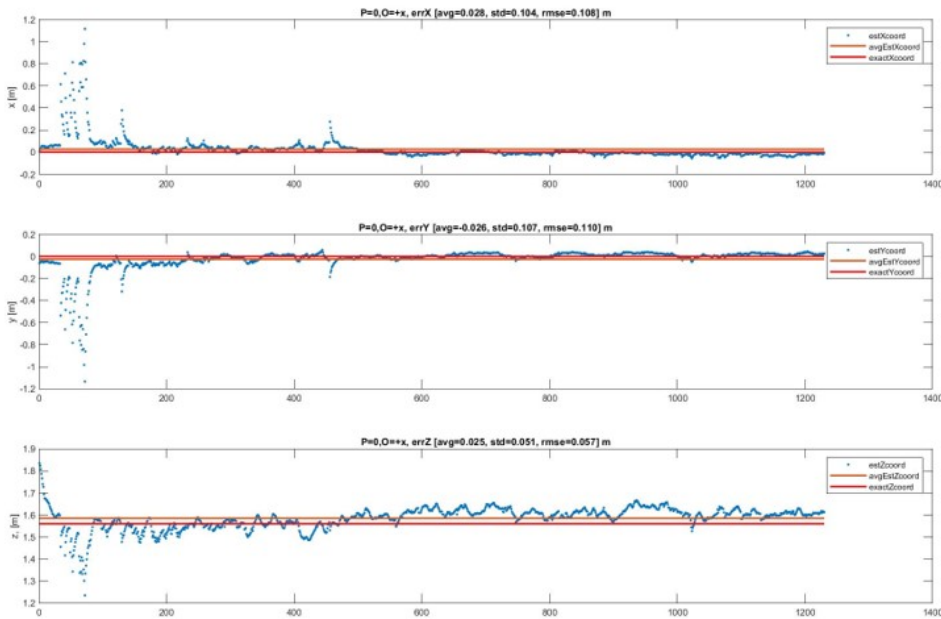


Figure 4.7: P model - 1 Tag on the right shoulder - Test point 0

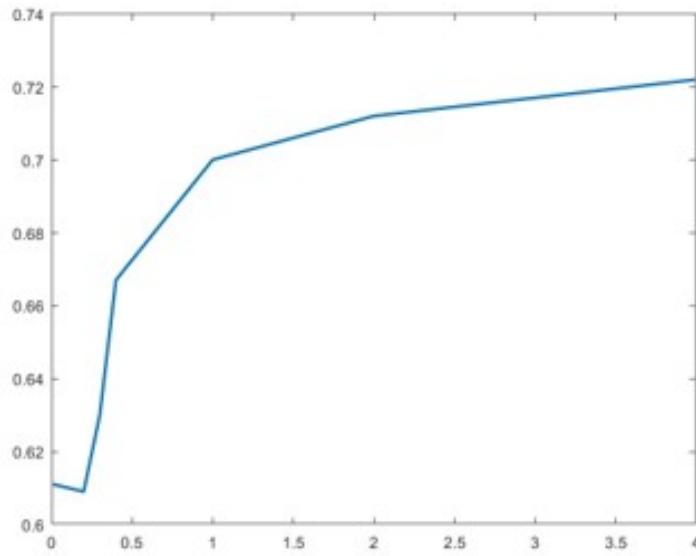


Figure 4.8: P model - 1 Tag on the right shoulder

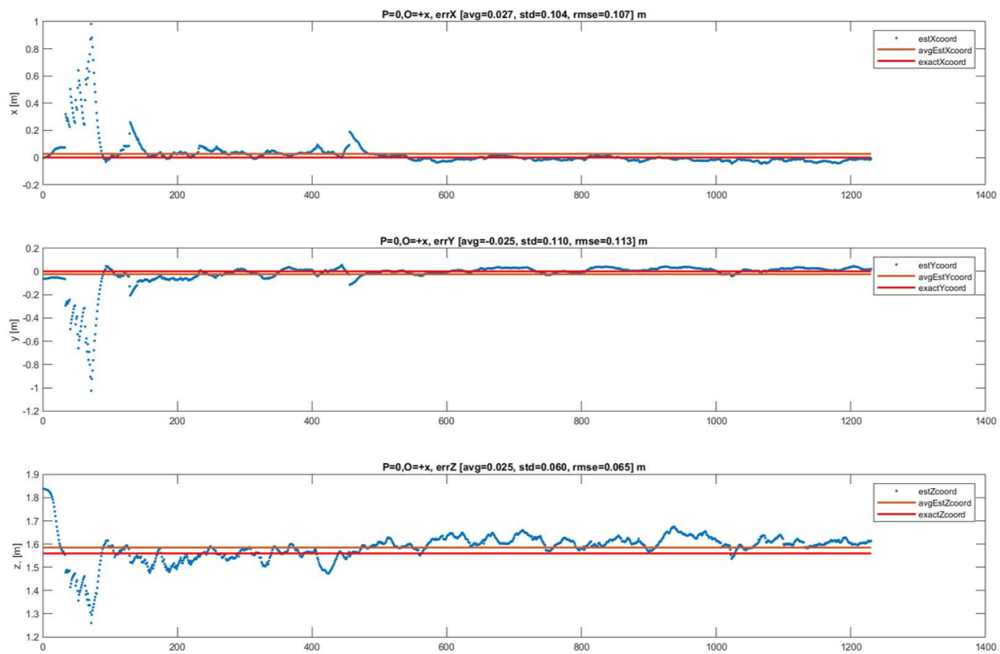


Figure 4.9: PV model - 1 Tag on the right shoulder

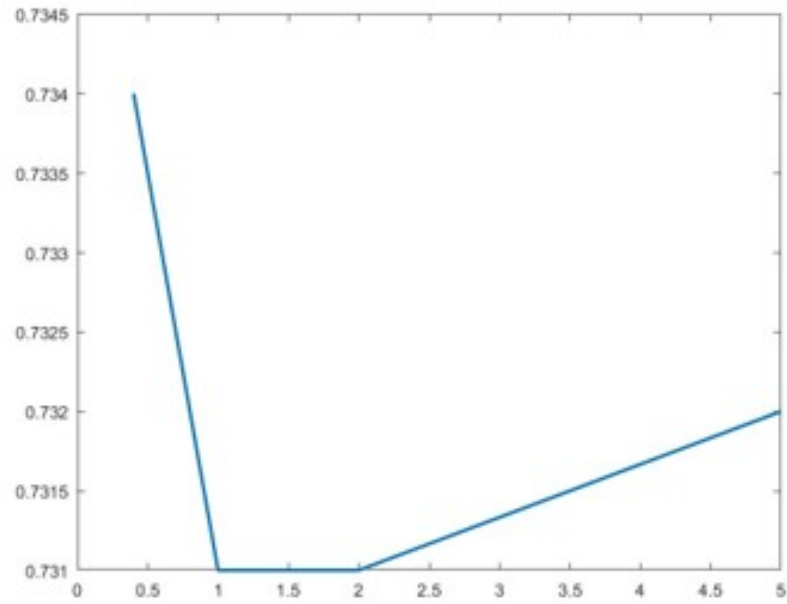


Figure 4.10: PV model - 1 Tag on the right shoulder

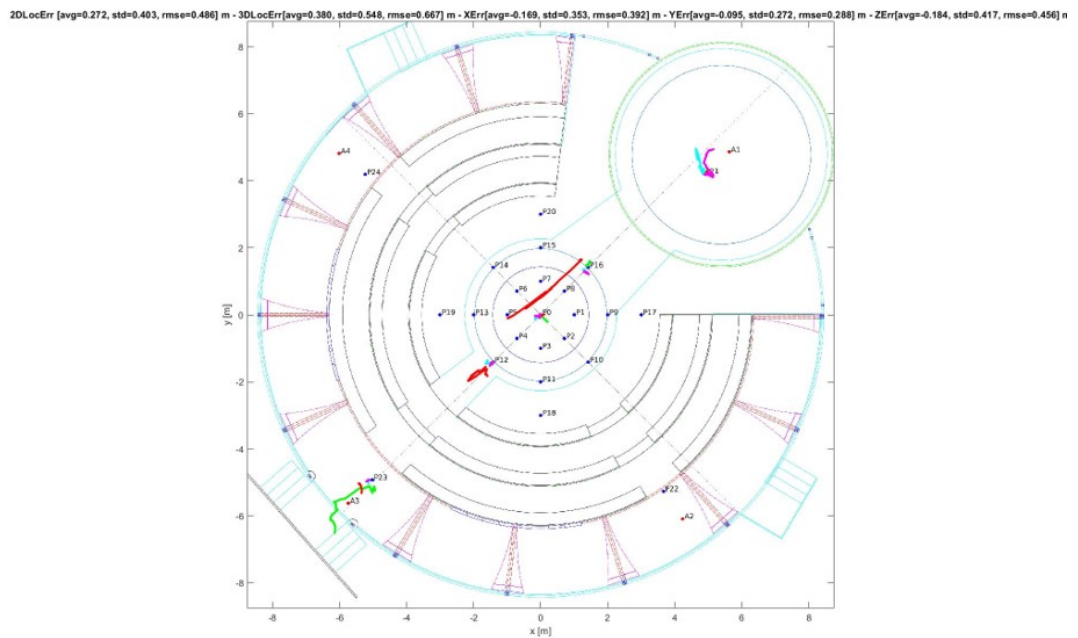


Figure 4.11: P model - 1 Tag on the right shoulder

Performance	
2DLocErr	[avg=0.272, std=0.403, RMS=0.486] m
3DLocErr	[avg=0.380, std=0.548, RMS=0.667] m
XErr	[avg=-0.169, std=0.353, RMS=0.392] m
YErr	[avg=-0.095, std=0.272, RMS=0.288] m
ZErr	[avg=-0.184, std=0.417, RMS=0.456] m

Table 4.3: Performance of $\sigma_a = 0.01$ for P model

As result, P model for tag on right shoulder has better performance comparing with PV model, by looking at Table 4.3 error for 3D localization is 0.667 when $\sigma_a = 0.01$, as shown in Figure 4.11. As result, the best performance for P model is when $\sigma_a = 0.01$, as shown in Figure 4.11 and Table 4.3

4.2.3 Dynamic Condition with Human Body – Tag on the right shoulder (walk)

4.2.3.1 P model

For mobility, by evaluation different σ_a for P model in EKF algorithm, smaller number of errors and the best performance is $\sigma_a = 4$, as shown in Figure 4.12. As result, in case of mobility the σ_a parameter should be increased.

4.2.3.2 PV model

For PV model, smaller number of errors and the best performance is $\sigma_a = 1.5$, as shown in Figure 4.13

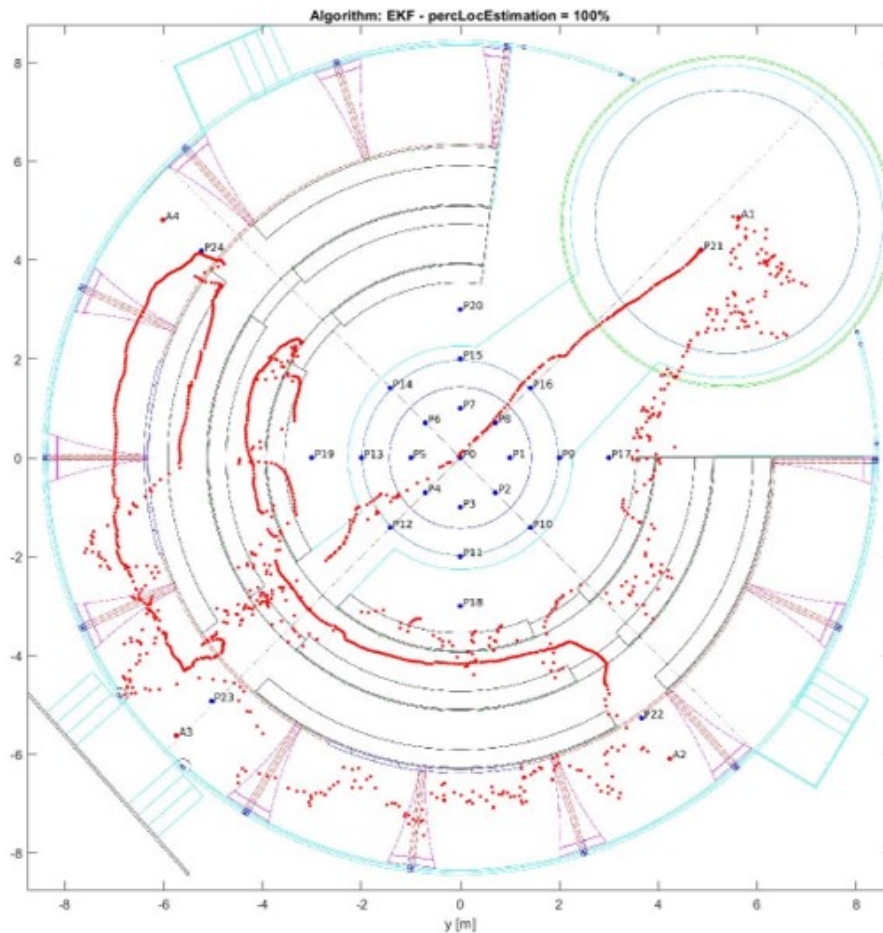


Figure 4.12: $\sigma_a = 4$, P model, walking by having 1 tag on right shoulder

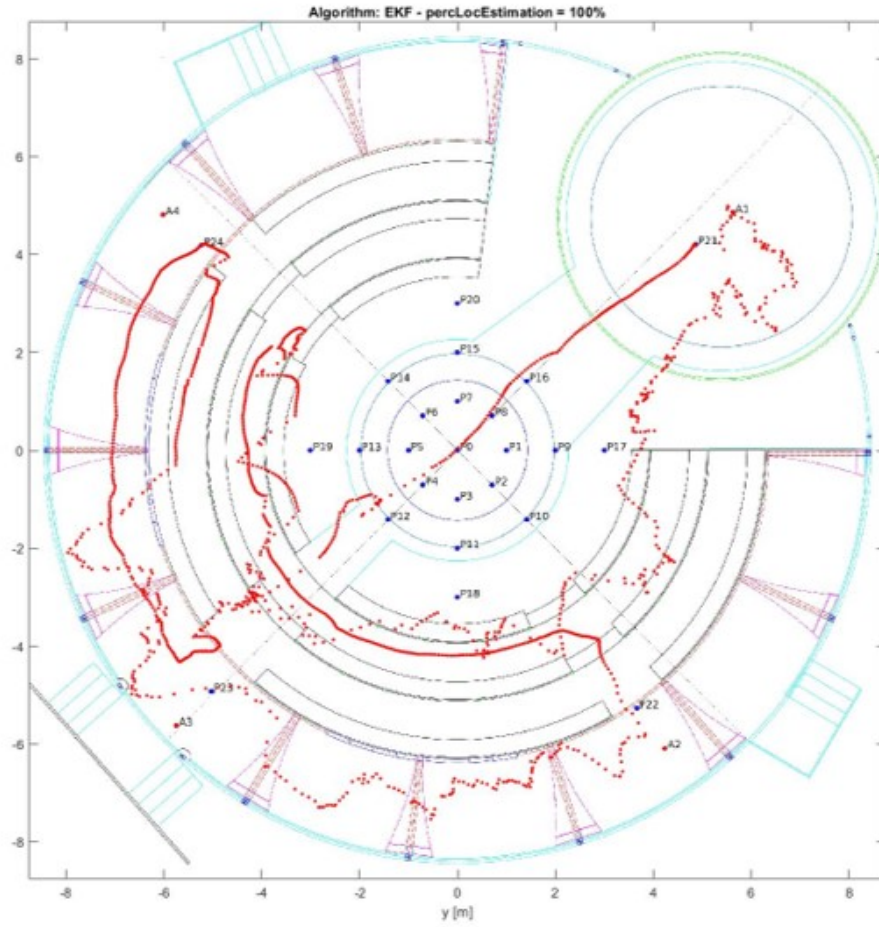


Figure 4.13: $\sigma_a = 1.5$, PV model, walking by having 1 tag on right shoulder

4.2.4 Dynamic Condition with Human Body – Tag on the right shoulder (run)

By looking at Figure 4.14 experiment has been done for P model in case of running when tag is on right shoulder.

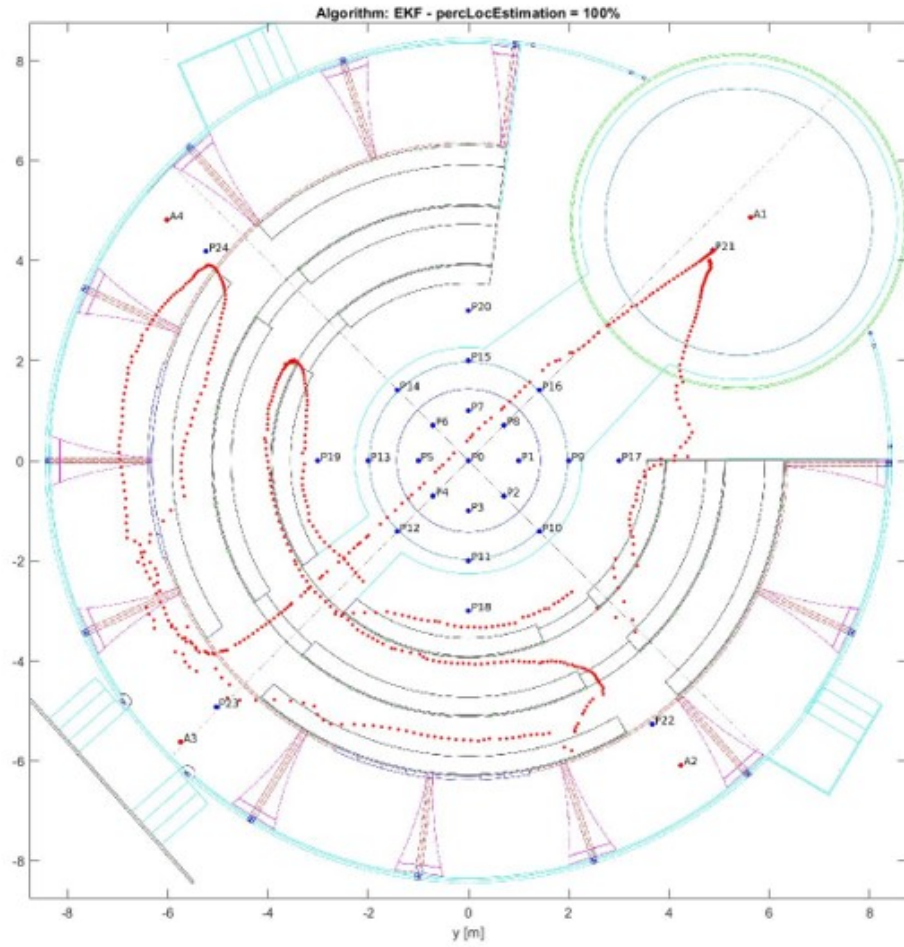


Figure 4.14: $\sigma_a = 4$, P model, tag on right shoulder while running

As shown in Figure 4.15, PV model in case of running with 1 tag on right shoulder.

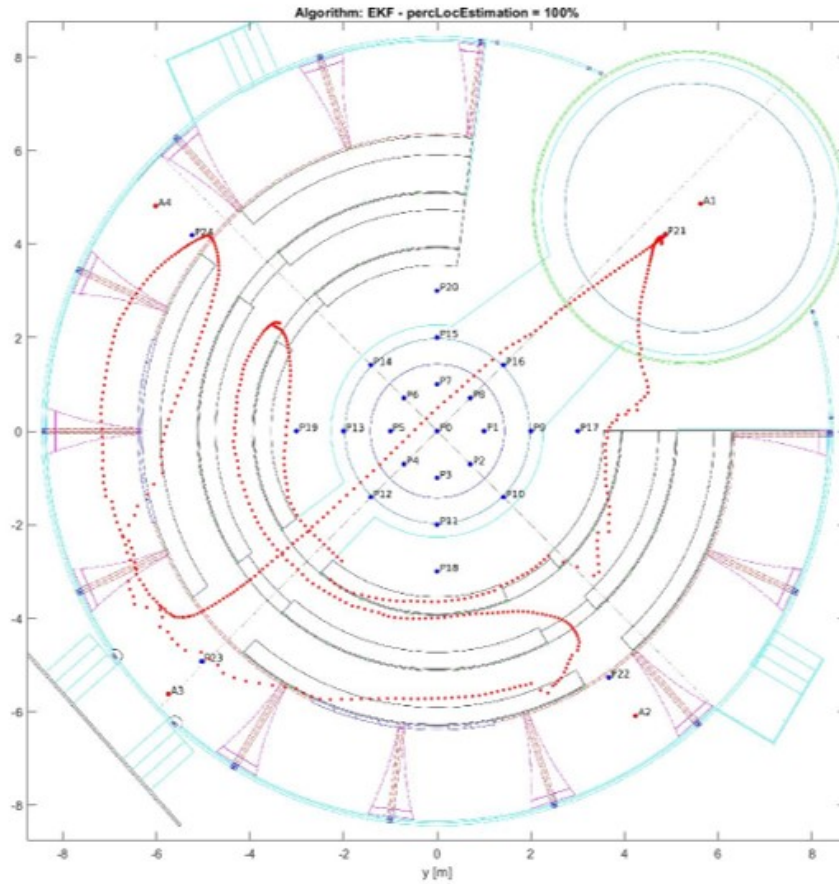


Figure 4.15: $\sigma_a = 1.5$, PV model in case of running by having 1 tag on right shoulder

4.2.5 Dynamic Condition with Human Body – Tag on the pocket (walk)

4.2.4.1 P model

For tracking in case of walking smaller number of errors and the best performance is when $\sigma_a = 4$ for P model, as shown in Figure 4.16

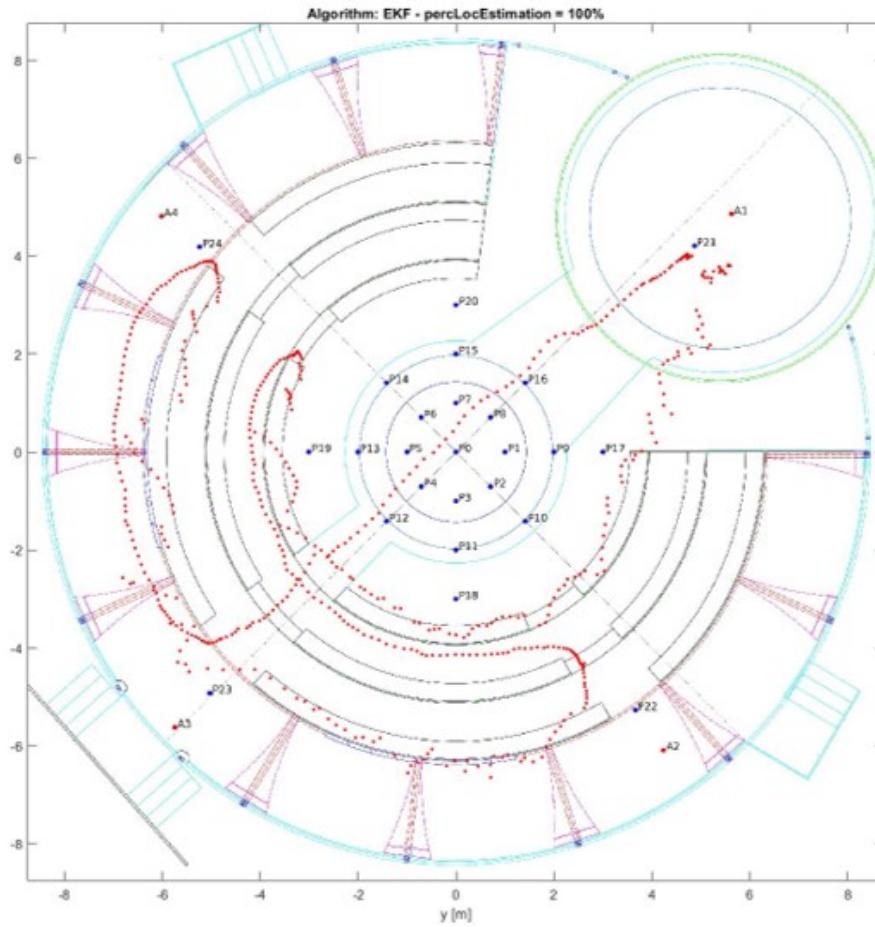


Figure 4.16: $\sigma_a = 4$, P model, walking by having 1 tag on the pocket

4.2.4.2 PV model

For PV model in case of walking, the best performance is when $\sigma_a = 1.5$, as shown in Figure 4.17

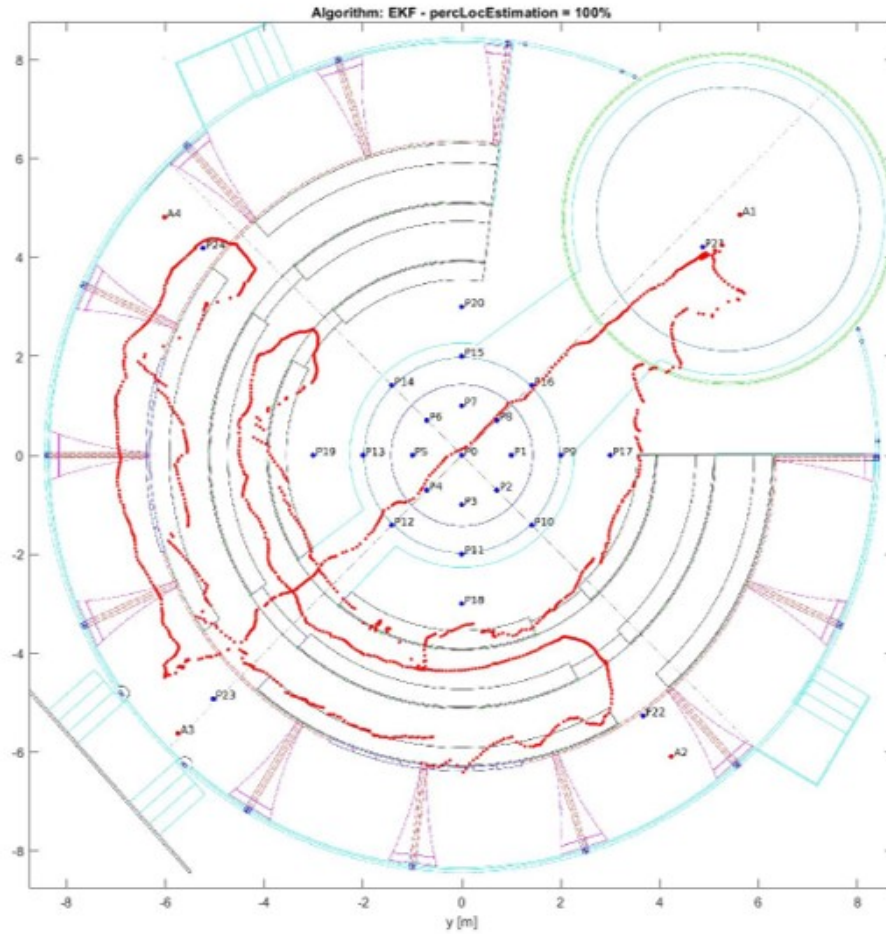


Figure 4.17: $\sigma_a = 1.5$, PV model, walking by having 1 tag on the pocket

4.2.6 Dynamic Condition with Human Body – Tag on the pocket (run)

As shown in Figure 4.18, this time previous experiment has been done in case of running when tag is on the right pocket.

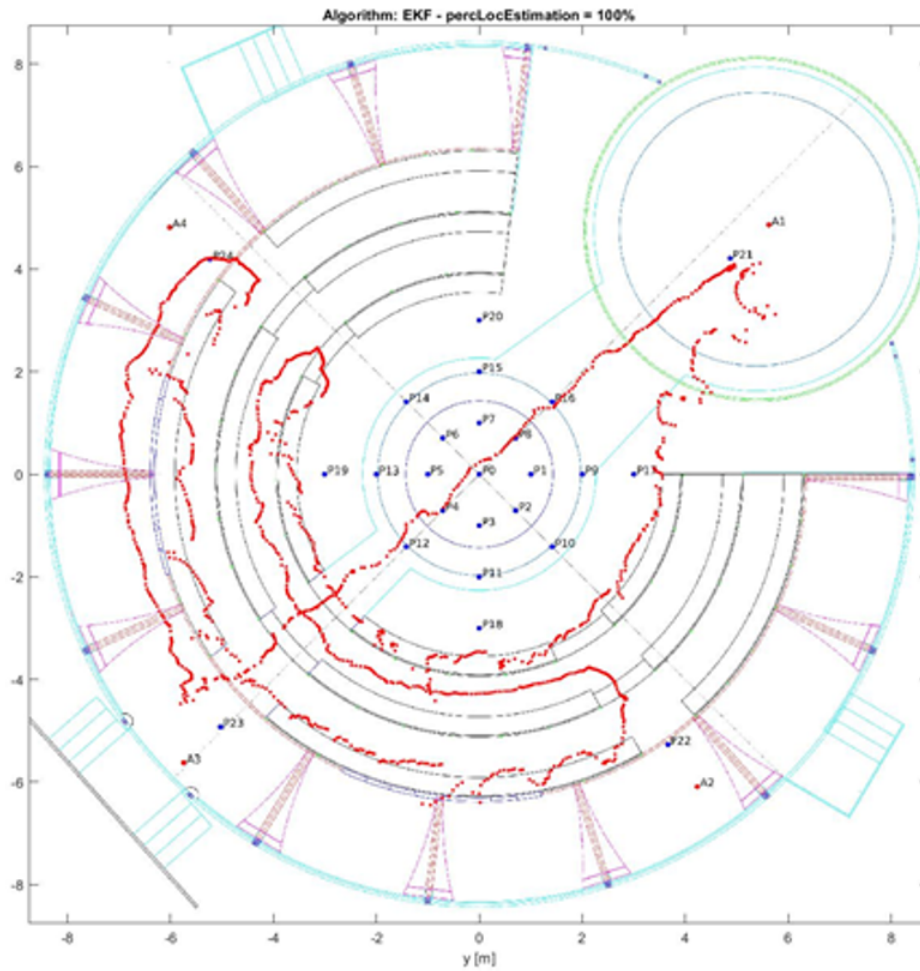


Figure 4.18: $\sigma_a = 4$, P model, running by having 1 tag on pocket

As shown in Figure 4.19, running by having one tag on the pocket in case of PV model.

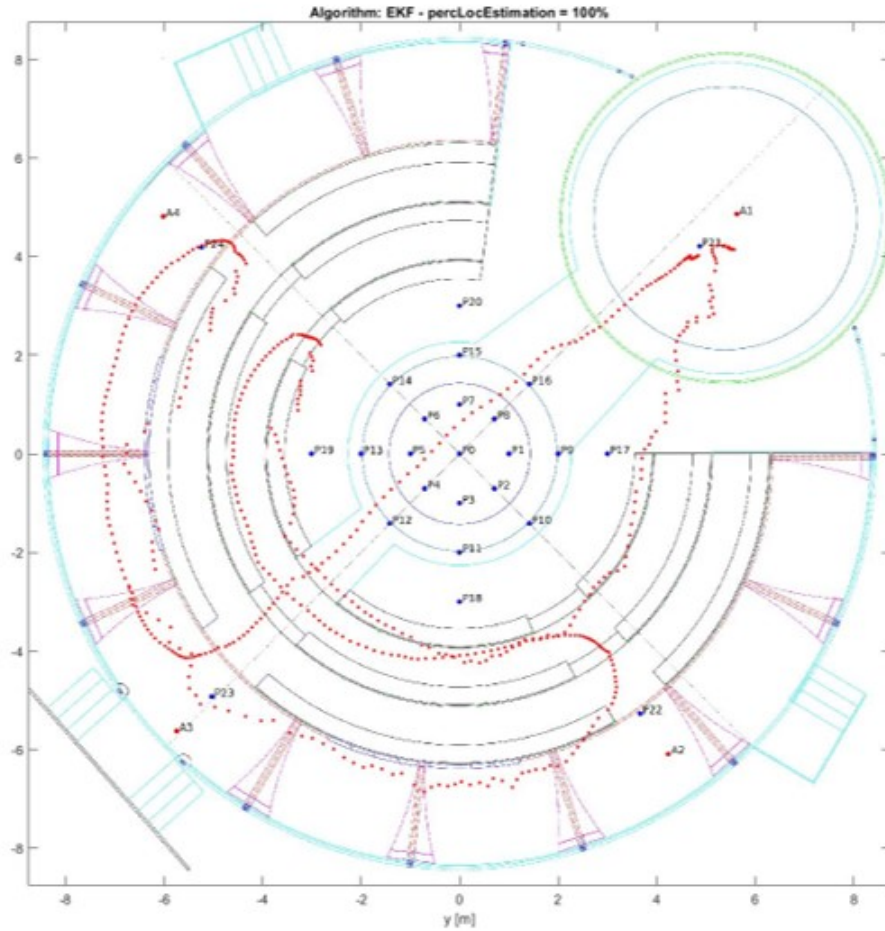


Figure 4.19: $\sigma_a = 1.5$, PV model, running by having 1 tag on pocket

4.2.7 Dynamic Condition with Human Body – Tag on the back belt (walk)

4.2.5.1 P model

For mobility, in case of walking, smaller number of errors and the best performance for P model is when $\sigma_a = 4$, as shown in Figure 4.20

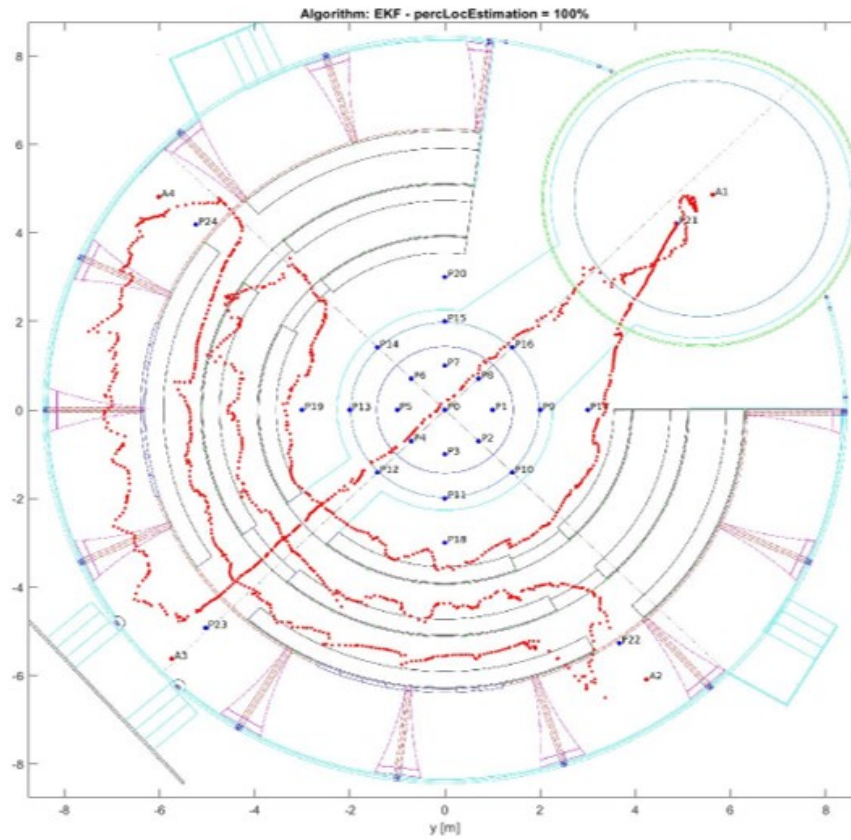


Figure 4.20: $\sigma_a=4$, P model, walking by having 1 tag on back belt

4.2.5.2 PV model

For mobility, in case of walking, smaller number of errors and the best performance for PV model is when $\sigma_a = 1.5$, as shown in Figure 4.21

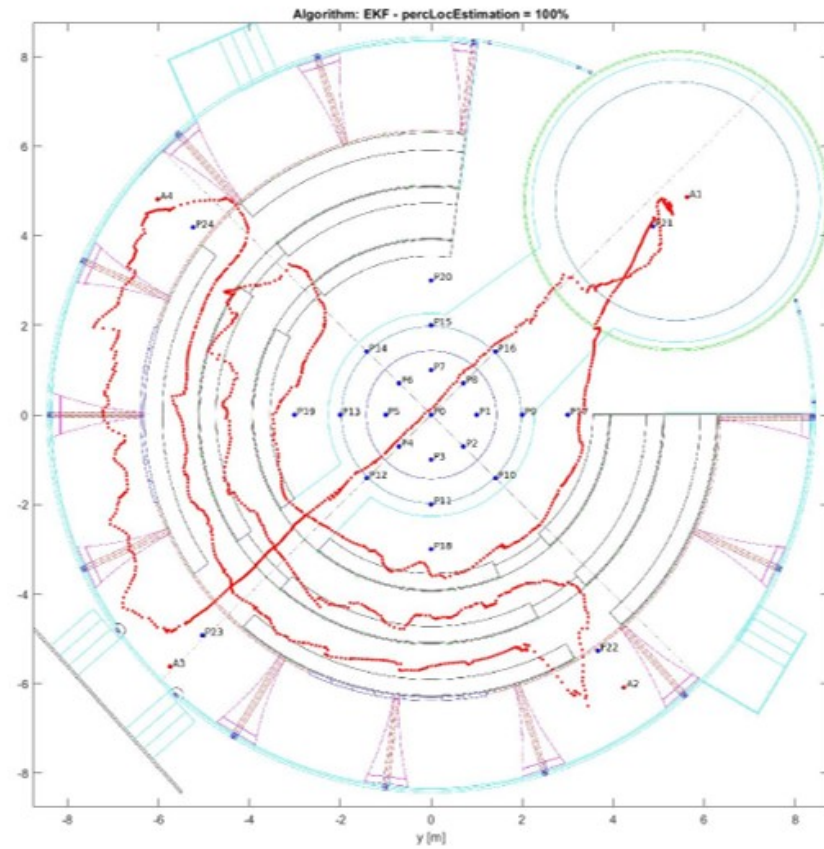


Figure 4.21: $\sigma_a = 1.5$, PV model, walking by having 1 tag on back belt

4.2.8 Dynamic Condition with Human Body – Tag on the back belt (run)

As shown in Figure 4.22 and 4.23, this time previous experiment has been done for running when tag is on back belt.

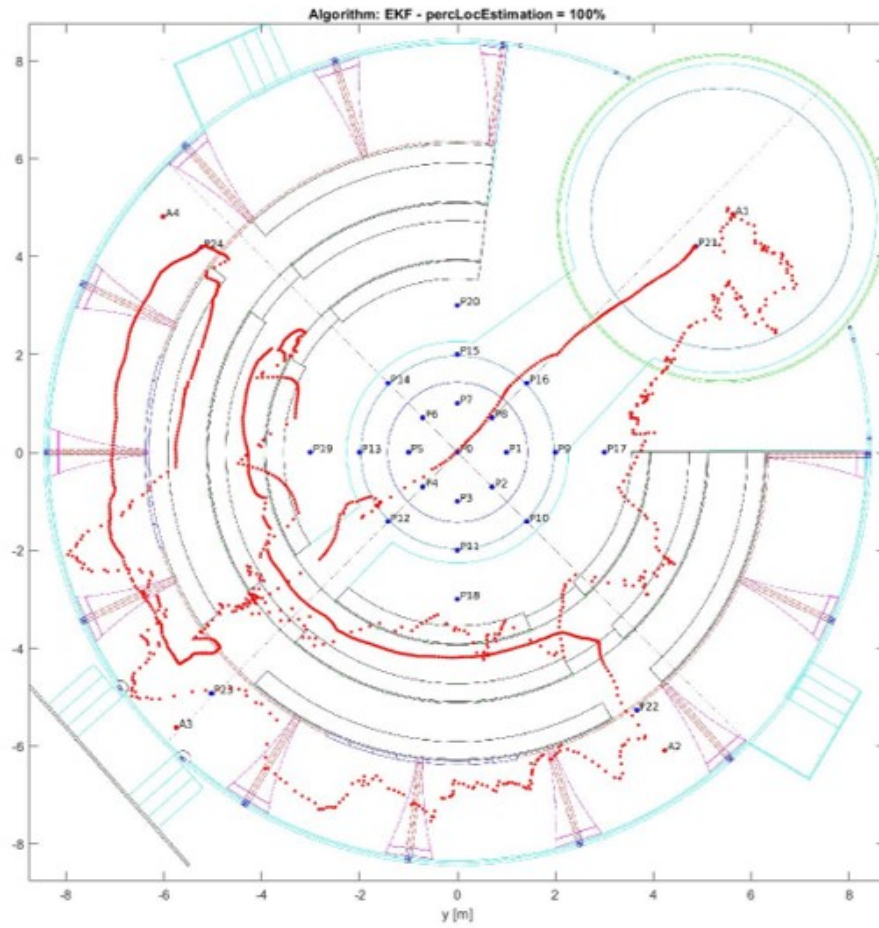


Figure 4.22: $\sigma_a = 4$, P model, running by having 1 tag on back belt

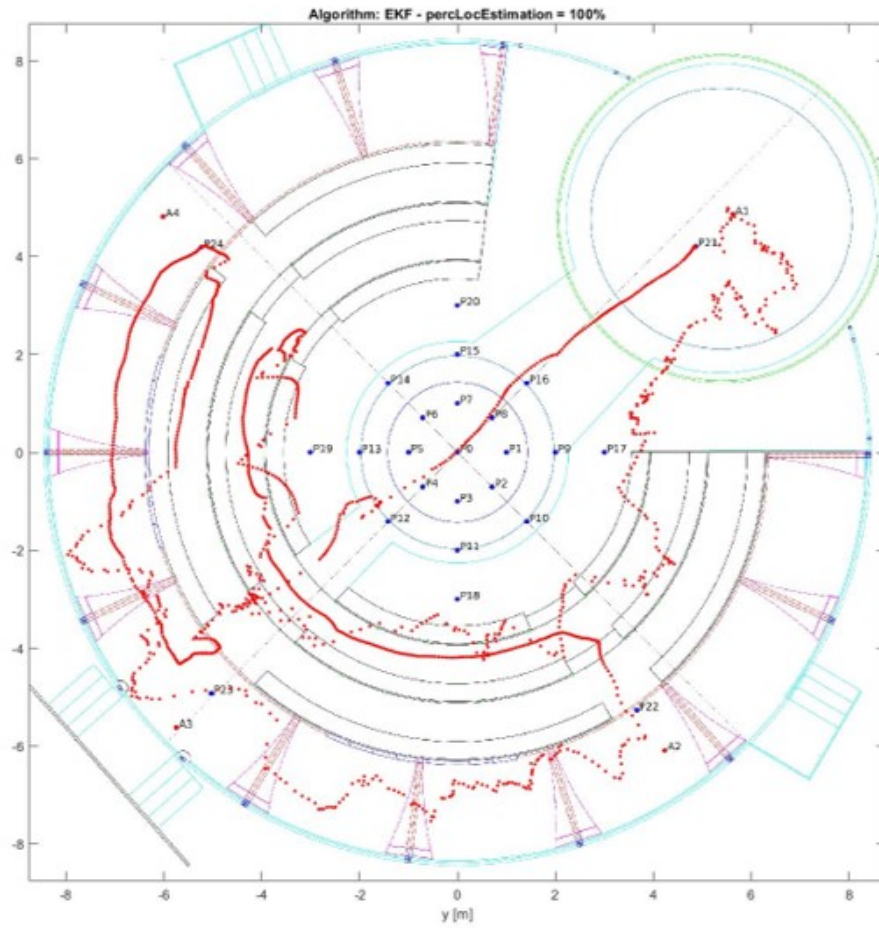


Figure 4.23: $\sigma_a = 1.5$, PV model, running by having 1 tag on back belt

Chapter 5

Design and Evaluation of the 3D Localization Algorithm - 2 Tags

5.1 Design of the EKF for 3D Localization for 2 Tags

EKF algorithm was simulated and tested in Matlab by having 2 Tags. The simulation allowed localization on right shoulder, right pocket and back belt as ranging measurements and then by using EKF localization algorithm, the best σ_a by having the best performance has been selected.

5.1.1 State Models

5.1.2.1 P model

As far as P model has two applications, estimate some measurement parameters knowing the exact position and tracking, where due to low sampling frequencies for instance, a dynamic model does not work well and a priori positions are predicted as random variables inside a certain region. \mathbf{Q}_k is presented as function of the time transurred between two measures Δ_T and the standard deviation σ_a of a Gaussian distributed acceleration vector. The state equation for 2 tags would be

$$\mathbf{x} = [x_1, y_1, z_1, x_2, y_2, z_2]^T \quad (5.1)$$

$$\mathbf{x}_k = f(\mathbf{x}_{k-1}, 0) = I_{6,6}\mathbf{x}_{k-1} \quad (5.2)$$

$$\mathbf{Q}_k = [\Delta_T I_{6,6}] [\Delta_T I_{6,6}]^T \sigma_a^2 \quad (5.3)$$

5.1.2.2 PV model

PV model is a dynamic KF and assumes near constant velocity between the estimation intervals Δ_t . One differences comparing with having 1 tag is size of matrix. The size of I matrix for 2 tags is $I_{6,6}$ which means it is two times bigger than having 1 tag. The state equation for 2 tags would be

$$\mathbf{x} = [x_1, y_1, z_1, x_2, y_2, z_2, v_{x_1}, v_{y_1}, v_{z_1}, v_{x_2}, v_{y_2}, v_{z_2}]^T \quad (5.4)$$

$$\mathbf{x}_k = F(\mathbf{x}_{k-1}, 0) = \begin{bmatrix} I_{6,6} & \Delta_T I_{6,6} \\ O_{6,6} & I_{6,6} \end{bmatrix} \mathbf{x}_{k-1} \quad (5.5)$$

$$\mathbf{Q}_k = \begin{bmatrix} 1/2 \Delta_T^2 I_{6,6} \\ \Delta_T I_{6,6} \end{bmatrix} \begin{bmatrix} 1/2 \Delta_T^2 I_{6,6} \\ \Delta_T I_{6,6} \end{bmatrix}^T \sigma_a^2 \quad (5.6)$$

5.1.2 Measurement Model

After evaluation of 3D localization algorithm for 1 Tag, the same evaluation has been done for two tags. z_k shows the number of distance estimates from each of these 2 tags. N and M define the number of distances from tag 1 and tag 2 respectively, as shown in formula 5.7

$$\mathbf{z}_k = [z_{T_1, A_1, k}, z_{T_1, A_2, k}, \dots, z_{T_1, A_N, k}, z_{T_2, A_1, k}, z_{T_2, A_2, k}, \dots, z_{T_2, A_M, k}]^T \quad (5.7)$$

For linearization of transformation between distances and coordinates, $h(\mathbf{x}_k)$ is used. First for linearization of transformation between distances and coordinates, $h(\mathbf{x}_1, k)$ is calculated for tag 1, as shown in formula 5.8 and then same calculation has been done for tag 2, $h(\mathbf{x}_2, k)$, as shown in Formula 5.9. As result, Formula 5.10 shows the result for both tags.

$$h(\mathbf{x}_{1,k}) = \begin{bmatrix} \sqrt{(x_{1,k} - x_{A_1})^2 + (y_{1,k} - y_{A_1})^2 + (z_{1,k} - z_{A_1})^2} \\ \sqrt{(x_{1,k} - x_{A_2})^2 + (y_{1,k} - y_{A_2})^2 + (z_{1,k} - z_{A_2})^2} \\ \vdots \\ \sqrt{(x_{1,k} - x_{A_N})^2 + (y_{1,k} - y_{A_N})^2 + (z_{1,k} - z_{A_N})^2} \end{bmatrix} \quad (5.8)$$

$$h(\mathbf{x}_{2,k}) = \begin{bmatrix} \sqrt{(x_{2,k} - x_{A_1})^2 + (y_{2,k} - y_{A_1})^2 + (z_{2,k} - z_{A_1})^2} \\ \sqrt{(x_{2,k} - x_{A_2})^2 + (y_{2,k} - y_{A_2})^2 + (z_{2,k} - z_{A_2})^2} \\ \vdots \\ \sqrt{(x_{2,k} - x_{A_M})^2 + (y_{2,k} - y_{A_M})^2 + (z_{2,k} - z_{A_M})^2} \end{bmatrix} \quad (5.9)$$

$$h(\mathbf{x}_k) = \begin{bmatrix} h(\mathbf{x}_{1,k}) \\ h(\mathbf{x}_{2,k}) \end{bmatrix} \quad (5.10)$$

For calculating \mathbf{H}_k , by having \hat{d} for 2 different tags, \mathbf{H}_k for first tag and second tag was evaluated, as shown in formula 5.11 and 5.12, respectively.

\mathbf{H}_k for P model, is a matrix with 6 rows that consist of 3 rows of zero, as shown in Formula 5.13. For PV model \mathbf{H}_k is a matrix of 12 rows and size of zero matrix is Nx9, as shown in Formula 5.14

$$H_{1,k} = \begin{bmatrix} \frac{x_{1,k} - x_{A_1}}{\hat{d}_{T_1,A_1,k}} & \frac{y_{1,k} - y_{A_1}}{\hat{d}_{T_1,A_1,k}} & \frac{z_{1,k} - z_{A_1}}{\hat{d}_{T_1,A_1,k}} \\ \frac{x_{1,k} - x_{A_2}}{\hat{d}_{T_1,A_2,k}} & \frac{y_{1,k} - y_{A_2}}{\hat{d}_{T_1,A_2,k}} & \frac{z_{1,k} - z_{A_2}}{\hat{d}_{T_1,A_2,k}} \\ \vdots & \vdots & \vdots \\ \frac{x_{1,k} - x_{A_N}}{\hat{d}_{T_1,A_N,k}} & \frac{y_{1,k} - y_{A_N}}{\hat{d}_{T_1,A_N,k}} & \frac{z_{1,k} - z_{A_N}}{\hat{d}_{T_1,A_N,k}} \end{bmatrix} \quad (5.11)$$

$$H_{2,k} = \begin{bmatrix} \frac{x_{2,k} - x_{A_1}}{\hat{d}_{T_2,A_1,k}} & \frac{y_{2,k} - y_{A_1}}{\hat{d}_{T_2,A_1,k}} & \frac{z_{2,k} - z_{A_1}}{\hat{d}_{T_2,A_1,k}} \\ \frac{x_{2,k} - x_{A_2}}{\hat{d}_{T_2,A_2,k}} & \frac{y_{2,k} - y_{A_2}}{\hat{d}_{T_2,A_2,k}} & \frac{z_{2,k} - z_{A_2}}{\hat{d}_{T_2,A_2,k}} \\ \vdots & \vdots & \vdots \\ \frac{x_{2,k} - x_{A_M}}{\hat{d}_{T_2,A_M,k}} & \frac{y_{2,k} - y_{A_M}}{\hat{d}_{T_2,A_M,k}} & \frac{z_{2,k} - z_{A_M}}{\hat{d}_{T_2,A_M,k}} \end{bmatrix} \quad (5.12)$$

$$\mathbf{H}_k = \begin{bmatrix} H_{1,k} & O_{N,3} \\ O_{M,3} & H_{2,k} \end{bmatrix} \quad (5.13)$$

$$\mathbf{H}_k = \begin{bmatrix} H_{1,k} & O_{N,3} & O_{N,3} \\ O_{M,3} & H_{2,k} & O_{M,3} \end{bmatrix} \quad (5.14)$$

5.2 Evaluation of the Localization Performance and Optimization

By having 2 tags on right shoulder, right pocket and back belt, performance of P model and PV model are evaluated and then by choosing the best σ_a for each of these models, the best performance with smaller number of errors was evaluated. To begin with, we consider 2 tags on right shoulder, on right pocket and in back belt.

5.2.1 Static Condition with Human Body – 2 Tags on the right shoulder

5.2.2.1 P model

When 2 tags are on right shoulder then different value for σ_a (as one parameter of Q_k matrix) were obtained, as shown in Figure 5.1. As conclusion, when $\sigma_a = 0.5$, rmse is 0.107 for P model, so performance is much better, as shown in Figure 5.2 and Table 5.1

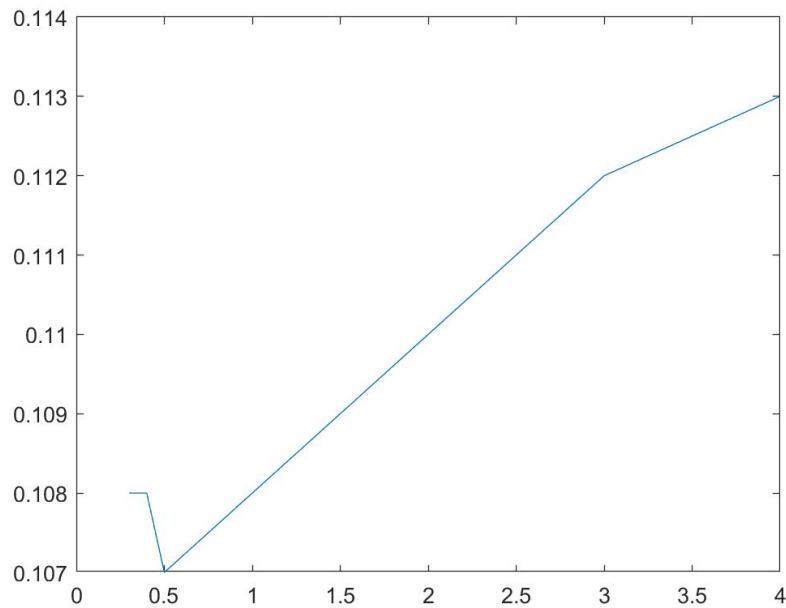


Figure 5.1: P model - ratio σ_a and rmse

Performance	
2DLocErr	[avg=0.085, std=0.032, RMS=0.091] m
3DLocErr	[avg=0.107, std=0.038, RMS=0.107] m
XErr	[avg=-0.063, std=0.043, RMS=0.076] m
YErr	[avg=-0.033, std=0.037, RMS=0.049] m
ZErr	[avg=-0.019, std=0.065, RMS=0.072] m

Table 5.1: 2 Tags - Performance of σ_a for P model

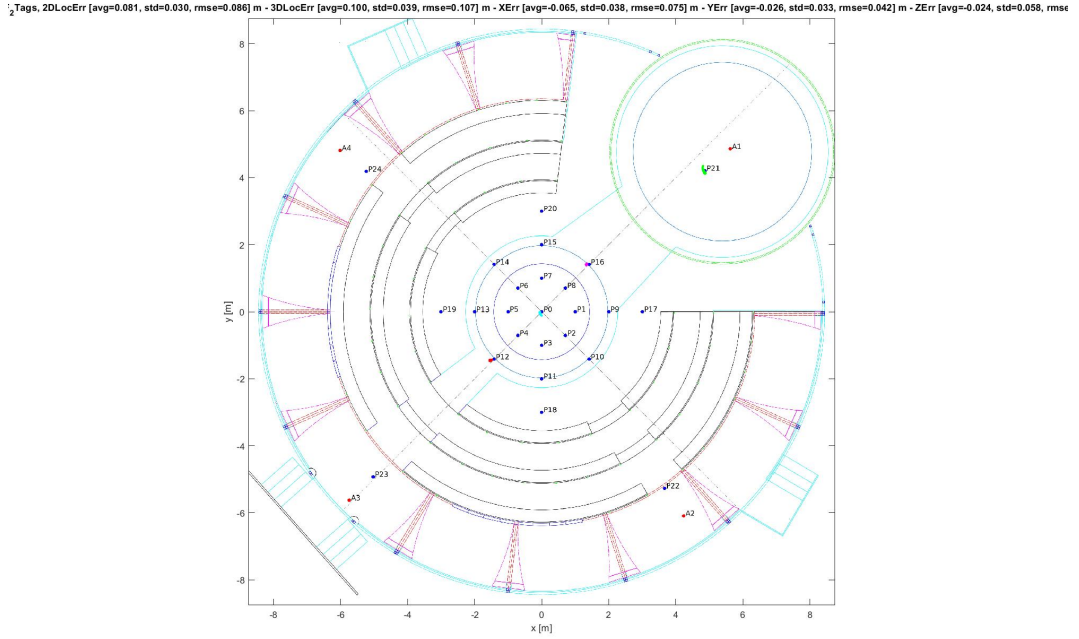


Figure 5.2: P model - 2 Tags on right shoulder

5.2.2.2 PV model

By considering different value of σ_a for PV model (as one parameter of \mathbf{Q}_k matrix), $\sigma_a = 0.01$ has the best performance, as shown in Figure 5.3 and Table 5.2

Performance	
2DLocErr	[avg=0.088, std=0.031, RMS=0.93] m
3DLocErr	[avg=0.103, std=0.034, RMS=0.109] m
XErr	[avg=-0.059, std=0.044, RMS=0.288] m
YErr	[avg=-0.038, std=0.042, RMS=0.057] m
ZErr	[avg=-0.010, std=0.056, RMS=0.063] m

Table 5.2: 2 Tags - Performance of σ_a for PV model

5.2.2 Static Condition with Human Body – 2 Tags on the Pocket

5.2.3.1 P model and PV model

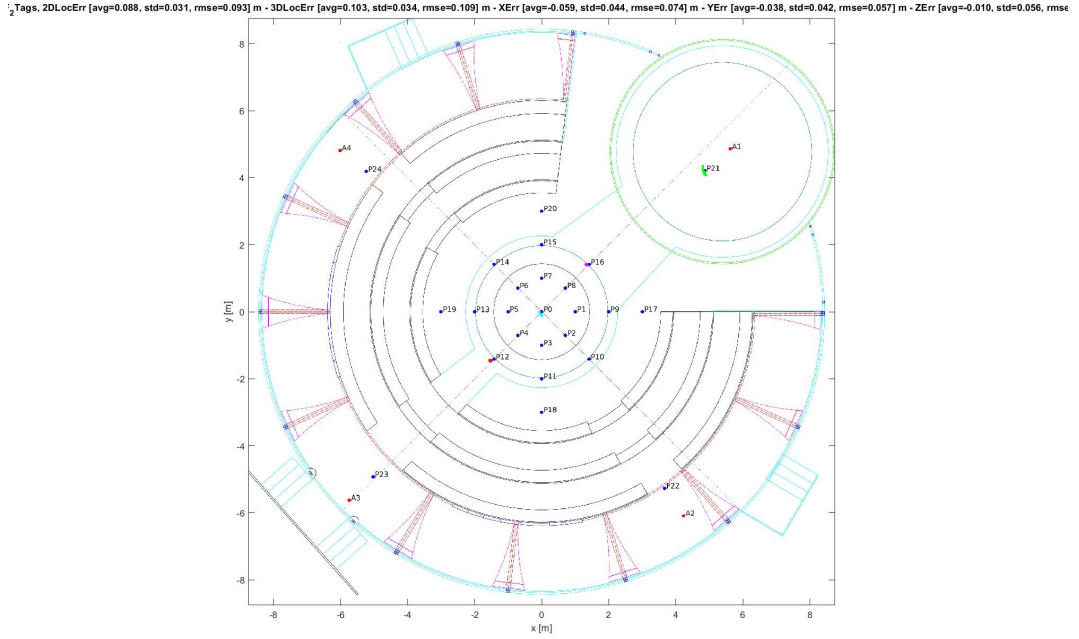


Figure 5.3: PV model - 2 Tags on right shoulder

We do not have any measurement for tag on the pocket

5.2.3 Static Condition with Human Body – 2 Tags on the Back Belt

5.2.4.1 P model

For P model in case of having 2 tags on back belt, the best performance is when $\sigma_a = 0.9$ by having $rmse = 0.360$, as shown in Figure 5.4 and table 5.3

Performance
2DLocErr [avg=0.168, std=0.102, RMS=0.196] m
3DLocErr [avg=0.352, std=0.076, RMS=0.360] m
XErr [avg=0.009, std=0.150, RMS=0.150] m
YErr [avg=-0.069, std=0.107, RMS=0.127] m
ZErr [avg=-0.268, std=0.139, RMS=0.168] m

Table 5.3: 2 Tags - Performance of σ_a for P model

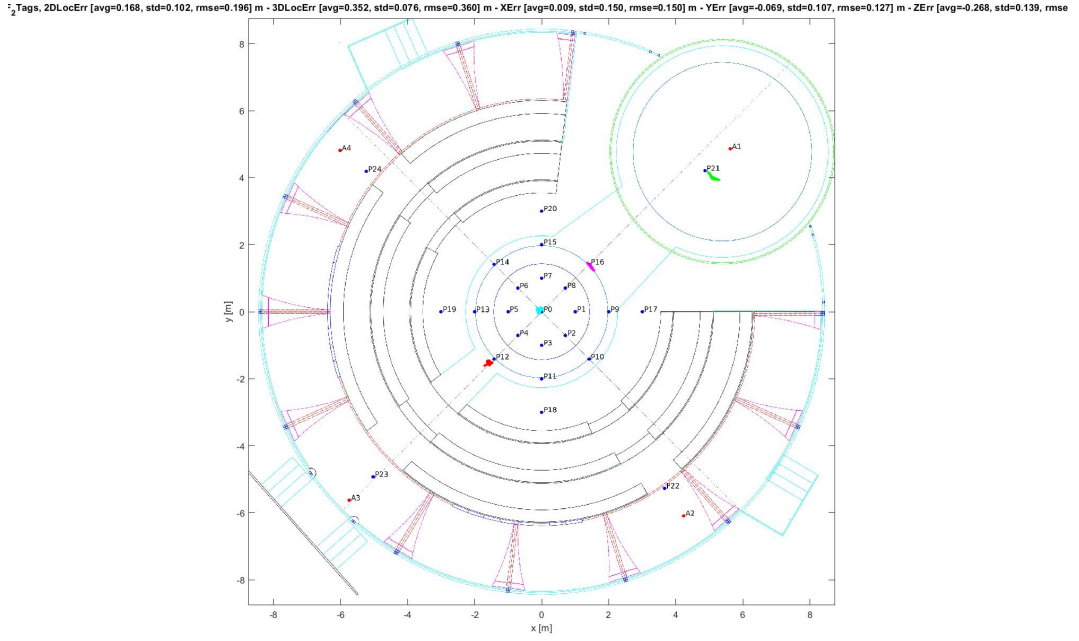


Figure 5.4: P model - 2 Tags on back belt

5.2.4.2 PV model

By having 2 tags on back belt for PV model, there will be $\sigma_a = 0.01$ as the best performance with $\text{rmse} = 0.361$, as shown in Figure 5.5 and Table 5.4. As result, rmse for tags on back belt is bigger than rmse for tags on right shoulder, so generally tags on right shoulder are better solution than back belt.

Performance	
2DLocErr	[avg=0.177, std=0.126, RMS=0.217] m
3DLocErr	[avg=0.347, std=0.097, RMS=0.361] m
XErr	[avg=0.021, std=0.162, RMS=0.163] m
YErr	[avg=-0.065, std=0.127, RMS=0.143] m
ZErr	[avg=-0.251, std=0.141, RMS=0.161] m

Table 5.4: 2 Tags - Performance of σ_a for PV model

$\bar{\sigma}_2$ Tags, 2DLocErr [avg=0.177, std=0.126, rmse=0.217] m - 3DLocErr [avg=0.347, std=0.097, rmse=0.361] m - XErr [avg=0.021, std=0.162, rmse=0.163] m - YErr [avg=-0.065, std=0.127, rmse=0.143] m - ZErr [avg=-0.251, std=0.141, rmse

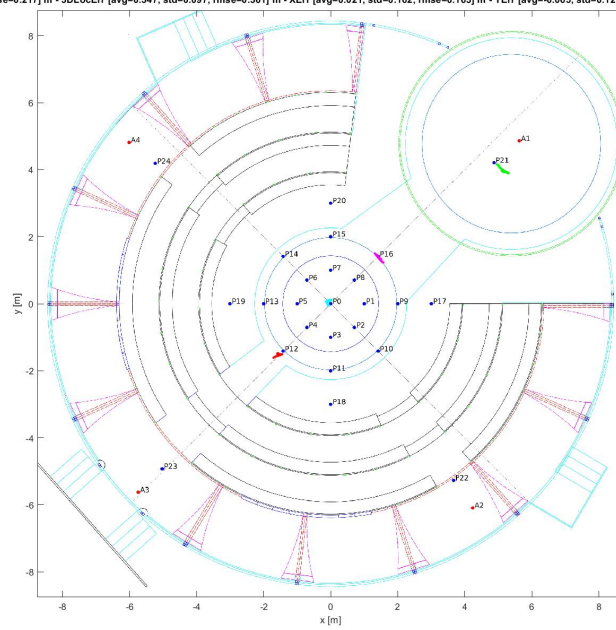


Figure 5.5: PV model - 2 Tags on back belt

Chapter 6

Design and Evaluation of the EKF for 3D Localization - 3 Tags

6.1 Design of the EKF for 3D Localization for 3 Tags

The simulation allowed localization with 3 tags, tags on right shoulder, right pocket and back belt. The EKF algorithm for 3 tags was simulated and tested in Matlab and at the end, the best performances for these different scenario are evaluated.

6.1.1 State Models

6.1.2.1 P model

P model has two applications, one is to filter and estimate some measurement parameters knowing the exact position; the second one is tracking, where due to low sampling frequencies for instance, a dynamic model does not work well and a priori positions are predicted as random variables inside a certain region. Q_k is presented as function of the time transcurrred between two measures Δ_T and the standard deviation σ_a of a Gaussian distributed acceleration vector. The state equation would be 6.2 and 6.3

By having 3 Tags on human body, I_{nn} will be a matrix of 9x9 as for each tag we have 3 position x, y and z, as shown in formula 6.1.

$$\mathbf{x} = [x_1, y_1, z_1, x_2, y_2, z_2, x_3, y_3, z_3]^T \quad (6.1)$$

$$\mathbf{x}_k = f(\mathbf{x}_{k-1}, 0) = I_{9,9}\mathbf{x}_{k-1} \quad (6.2)$$

$$\mathbf{Q}_k = [\Delta_T I_{9,9}] [\Delta_T I_{9,9}]^T \sigma_a^2 \quad (6.3)$$

6.1.2.2 PV model

PV model is a dynamic KF and assumes near constant velocity between the estimation intervals Δ_T . The state equation for 3 tags is shown in formula 6.4. Differences of x_k and \mathbf{Q}_k for 3 tags comparing with 1 tag is, matrix $I_{9,9}$ 3 times bigger than matrix $I_{3,3}$ for 1 tag, as shown in Formula 6.5 and 6.6

$$\mathbf{x} = [x_1, y_1, z_1, x_2, y_2, z_2, x_3, y_3, z_3, v_{x_1}, v_{y_1}, v_{z_1}, v_{x_2}, v_{y_2}, v_{z_2}, v_{x_3}, v_{y_3}, v_{z_3}]^T \quad (6.4)$$

$$\mathbf{x}_k = F(\mathbf{x}_{k-1}, 0) = \begin{bmatrix} I_{9,9} & \Delta_T I_{9,9} \\ O_{9,9} & I_{9,9} \end{bmatrix} \mathbf{x}_{k-1} \quad (6.5)$$

$$\mathbf{Q}_k = \begin{bmatrix} 1/2\Delta_T^2 I_{9,9} \\ \Delta_T I_{9,9} \end{bmatrix} \begin{bmatrix} 1/2\Delta_T^2 I_{9,9} \\ \Delta_T I_{9,9} \end{bmatrix}^T \sigma_a^2 \quad (6.6)$$

6.1.2 Measurement Model

After evaluation of 3D localization Algorithm for 2 Tags, simulation is continued by having 3 Tags. N estimating distances from tag 1, M number of distances from tag 2 and P number of distance measurements from tag 3, as shown in formula 6.7

$$\mathbf{z}_k = [z_{T_1,A_1,k}, z_{T_1,A_2,k}, \dots, z_{T_1,A_N,k}, \\ z_{T_2,A_1,k}, z_{T_2,A_2,k}, \dots, z_{T_2,A_M,k}, \\ z_{T_3,A_1,k}, z_{T_3,A_2,k}, \dots, z_{T_3,A_P,k}]^T \quad (6.7)$$

linearization of transformation between distances and coordinates has been evaluated for each of these 3 tags separately, as shown in formula 6.8, 6.9 and 6.10. As result, $h(x_k)$ is a matrix with 3 rows that each rows consist of these 3 tags linearization.

$$h(\mathbf{x}_{1,k}) = \begin{bmatrix} \sqrt{(x_{1,k} - x_{A_1})^2 + (y_{1,k} - y_{A_1})^2 + (z_{1,k} - z_{A_1})^2} \\ \sqrt{(x_{1,k} - x_{A_2})^2 + (y_{1,k} - y_{A_2})^2 + (z_{1,k} - z_{A_2})^2} \\ \vdots \\ \sqrt{(x_{1,k} - x_{A_N})^2 + (y_{1,k} - y_{A_N})^2 + (z_{1,k} - z_{A_N})^2} \end{bmatrix} \quad (6.8)$$

$$h(\mathbf{x}_{2,k}) = \begin{bmatrix} \sqrt{(x_{2,k} - x_{A_1})^2 + (y_{2,k} - y_{A_1})^2 + (z_{2,k} - z_{A_1})^2} \\ \sqrt{(x_{2,k} - x_{A_2})^2 + (y_{2,k} - y_{A_2})^2 + (z_{2,k} - z_{A_2})^2} \\ \vdots \\ \sqrt{(x_{2,k} - x_{A_M})^2 + (y_{2,k} - y_{A_M})^2 + (z_{2,k} - z_{A_M})^2} \end{bmatrix} \quad (6.9)$$

$$h(\mathbf{x}_{3,k}) = \begin{bmatrix} \sqrt{(x_{3,k} - x_{A_1})^2 + (y_{3,k} - y_{A_1})^2 + (z_{3,k} - z_{A_1})^2} \\ \sqrt{(x_{3,k} - x_{A_2})^2 + (y_{3,k} - y_{A_2})^2 + (z_{3,k} - z_{A_2})^2} \\ \vdots \\ \sqrt{(x_{3,k} - x_{A_P})^2 + (y_{3,k} - y_{A_P})^2 + (z_{3,k} - z_{A_P})^2} \end{bmatrix} \quad (6.10)$$

$$h(\mathbf{x}_k) = [h(\mathbf{x}_{1,k}) \quad h(\mathbf{x}_{2,k}) \quad h(\mathbf{x}_{3,k})] \quad (6.11)$$

For estimating value of \mathbf{H}_x , different \hat{d} for each of 3 tags is used (\hat{d} is result of $h(x_k)$ that evaluated in formula 6.11). Then by having \mathbf{H}_k for first tag (Formula 6.12), second tag (Formula 6.13) and third tag (Formula 6.14), \mathbf{H}_k of 3 tags for P model and PV model has been obtained.

$$H_{1,k} = \begin{bmatrix} \frac{x_{1,k} - x_{A_1}}{\hat{d}_{T_1,A_1,k}} & \frac{y_{1,k} - y_{A_1}}{\hat{d}_{T_1,A_1,k}} & \frac{z_{1,k} - z_{A_1}}{\hat{d}_{T_1,A_1,k}} \\ \frac{x_{1,k} - x_{A_2}}{\hat{d}_{T_1,A_2,k}} & \frac{y_{1,k} - y_{A_2}}{\hat{d}_{T_1,A_2,k}} & \frac{z_{1,k} - z_{A_2}}{\hat{d}_{T_1,A_2,k}} \\ \vdots & \vdots & \vdots \\ \frac{x_{1,k} - x_{A_N}}{\hat{d}_{T_1,A_N,k}} & \frac{y_{1,k} - y_{A_N}}{\hat{d}_{T_1,A_N,k}} & \frac{z_{1,k} - z_{A_N}}{\hat{d}_{T_1,A_N,k}} \end{bmatrix} \quad (6.12)$$

$$H_{2,k} = \begin{bmatrix} \frac{x_{2,k} - x_{A_1}}{\hat{d}_{T_2,A_1,k}} & \frac{y_{2,k} - y_{A_1}}{\hat{d}_{T_2,A_1,k}} & \frac{z_{2,k} - z_{A_1}}{\hat{d}_{T_2,A_1,k}} \\ \frac{x_{2,k} - x_{A_2}}{\hat{d}_{T_2,A_2,k}} & \frac{y_{2,k} - y_{A_2}}{\hat{d}_{T_2,A_2,k}} & \frac{z_{2,k} - z_{A_2}}{\hat{d}_{T_2,A_2,k}} \\ \vdots & \vdots & \vdots \\ \frac{x_{2,k} - x_{A_M}}{\hat{d}_{T_2,A_M,k}} & \frac{y_{2,k} - y_{A_M}}{\hat{d}_{T_2,A_M,k}} & \frac{z_{2,k} - z_{A_M}}{\hat{d}_{T_2,A_M,k}} \end{bmatrix} \quad (6.13)$$

$$H_{3,k} = \begin{bmatrix} \frac{x_{3,k} - x_{A_1}}{\hat{d}_{T_3,A_1,k}} & \frac{y_{3,k} - y_{A_1}}{\hat{d}_{T_3,A_1,k}} & \frac{z_{3,k} - z_{A_1}}{\hat{d}_{T_3,A_1,k}} \\ \frac{x_{3,k} - x_{A_2}}{\hat{d}_{T_3,A_2,k}} & \frac{y_{3,k} - y_{A_2}}{\hat{d}_{T_3,A_2,k}} & \frac{z_{3,k} - z_{A_2}}{\hat{d}_{T_3,A_2,k}} \\ \vdots & \vdots & \vdots \\ \frac{x_{3,k} - x_{A_P}}{\hat{d}_{T_3,A_P,k}} & \frac{y_{3,k} - y_{A_P}}{\hat{d}_{T_3,A_P,k}} & \frac{z_{3,k} - z_{A_P}}{\hat{d}_{T_3,A_P,k}} \end{bmatrix} \quad (6.14)$$

\mathbf{H}_k for P model is a Nx9 matrix while for PV model the size of matrix is Nx18, as shown in formula 6.15 and 6.16

$$\mathbf{H}_k = \begin{bmatrix} H_{1,k} & O_{N,3} & O_{N,3} \\ O_{M,3} & H_{2,k} & O_{M,3} \\ O_{P,3} & O_{P,3} & H_{3,k} \end{bmatrix} \quad (6.15)$$

$$\mathbf{H}_k = \begin{bmatrix} H_{1,k} & O_{N,3} & O_{N,3} & O_{N,3} & O_{N,3} & O_{N,3} \\ O_{M,3} & H_{2,k} & O_{M,3} & O_{M,3} & O_{M,3} & O_{M,3} \\ O_{P,3} & O_{P,3} & H_{3,k} & O_{P,3} & O_{P,3} & O_{P,3} \end{bmatrix} \quad (6.16)$$

6.2 Evaluation of the Localization Performance and Optimization

By having three tags on right shoulder, right pocket and back belt, performance of P model and PV model are evaluated and then by choosing the best σ_a for P model and PV model for right shoulder, right pocket and back belt, the best scenario by having smaller number of errors is selected. To begin with, tag on right shoulder is considered, after that right pocket and at the end back belt have been taken into consideration.

6.2.1 Static Condition with Human Body – Tag on the Shoulder

6.2.2.1 P model

By having 3 tags and evaluating different value of σ_a (as one parameter of \mathbf{Q}_k matrix in our EKF algorithm) for each of them rmse is obtained.

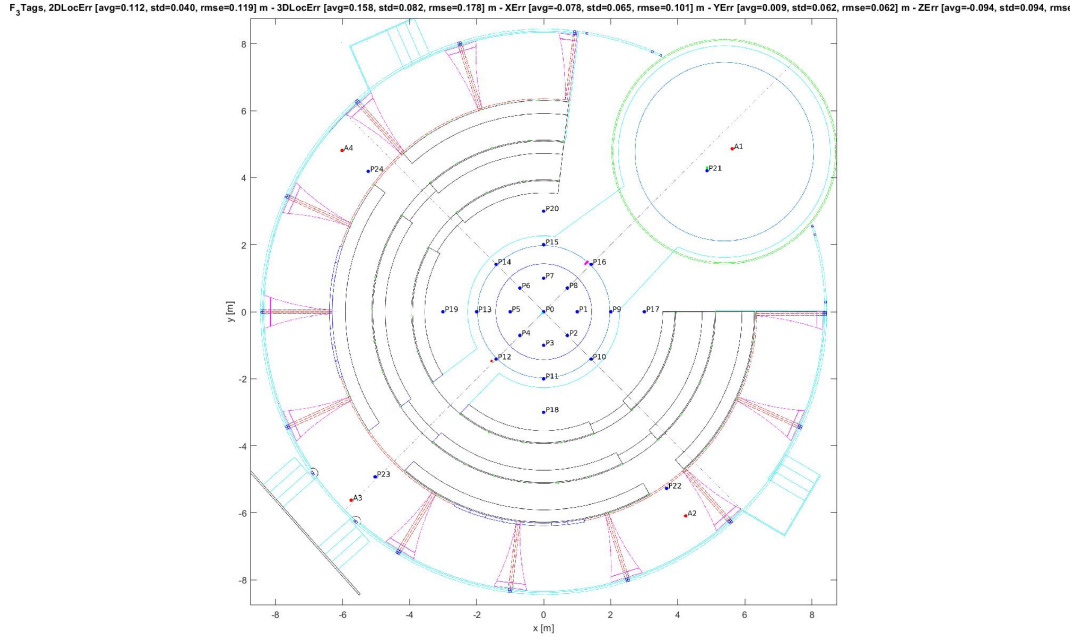


Figure 6.1: P model - 3 Tags on right shoulder

Performance
2DLocErr [avg=0.112, std=0.040, RMS=0.119] m
3DLocErr [avg=0.158, std=0.082, RMS=0.134] m
XErr [avg=-0.078, std=0.065, RMS=0.101] m
YErr [avg=0.009, std=0.062, RMS=0.062] m
ZErr [avg=-0.094, std=0.094, RMS=0.094] m

Table 6.1: 3 Tags - Performance of σ_a for P model

The best performance is for P model when tags are on right shoulder and $\sigma_a = 3.5$, as shown in Figure 6.1 and Table 6.1.

6.2.2.2 PV model

By evaluating different value of σ_a (as one parameter of Q_k matrix in EKF algorithm), different value of rmse has been obtained.

As a result, the best performance for PV model by having tags on right shoulder is when $\sigma_a = 3$, as shown in Table 6.2

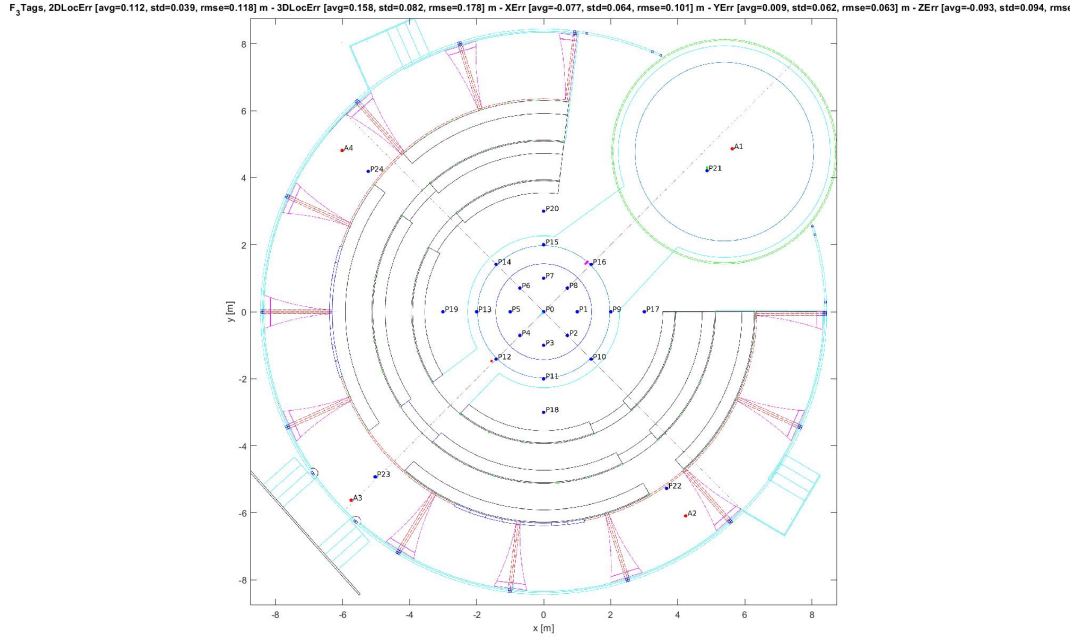


Figure 6.2: PV model - 3 Tags on right shoulder

Performance	
2DLocErr	[avg=0.112, std=0.039, RMS=0.118] m
3DLocErr	[avg=0.158, std=0.082, RMS=0.137] m
XErr	[-avg=0.077, std=0.064, RMS=0.101] m
YErr	[avg=0.009, std=0.062, RMS=0.063] m
ZErr	[avg=-0.093, std=0.094, RMS=0.094] m

Table 6.2: 3 Tags - Performance of σ_a for PV model

6.2.2 Static Condition with Human Body – Tag on the Pocket

6.2.3.1 P model and PV model

There is no measurement

6.2.3 Static Condition with Human Body – Tag on the Back Belt

6.3.4.1 P model

By evaluating different value of σ_a (as one parameter of \mathbf{Q}_k matrix in EKF algorithm) different value of rmse can be seen, as shown in Figure 6.3

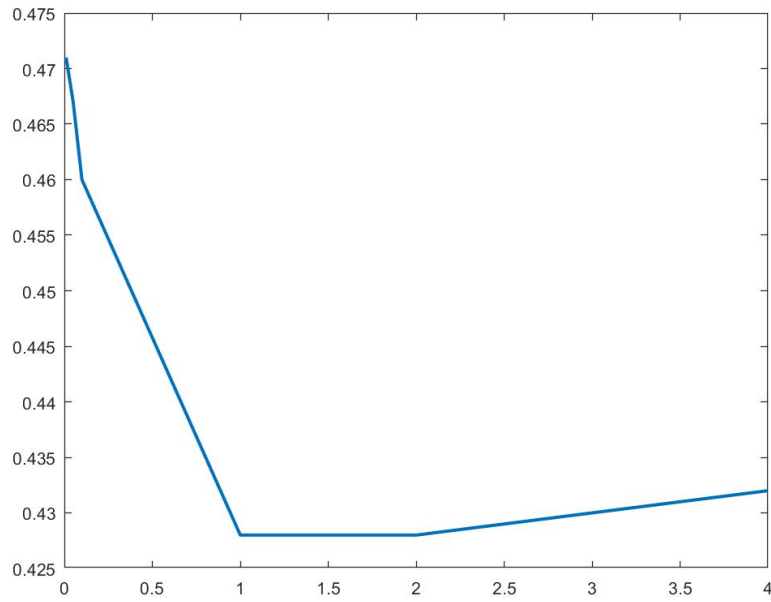


Figure 6.3: Ratio between σ_a and rmse as a function of σ_a

Performance	
2DLocErr	[avg=0.175, std=0.104, RMS=0.203] m
3DLocErr	[avg=0.419, std=0.090, RMS=0.428] m
XErr	[avg=0.054, std=0.068, RMS=0.086] m
YErr	[avg=0.149, std=0.108, RMS=0.184] m
ZErr	[avg=-0.336, std=0.171, RMS=0.191] m

Table 6.3: 3 Tags - Performance of σ_a for P model

The best performance for right shoulder for P model is when $\sigma_a = 2$, as shown in Figure 6.4 and Table 6.3

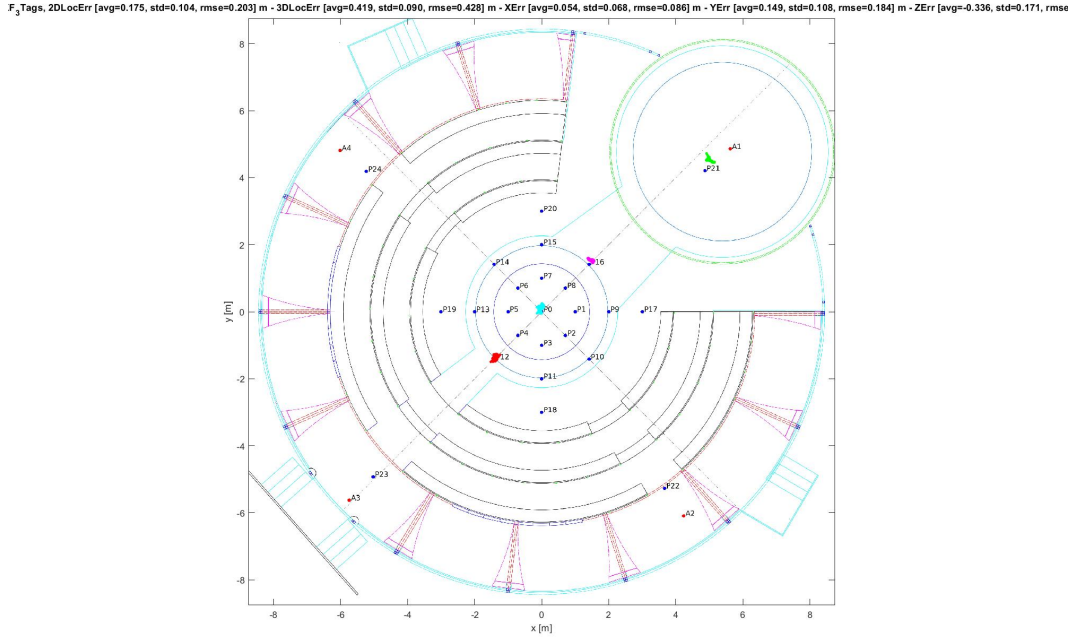


Figure 6.4: P model - 3 Tags on back belt

6.3.4.2 PV model

By evaluating different value of σ_a (as one parameter of Q_k matrix in EKF algorithm for 3 Tags) different value of rmse were obtained, as shown in Figure 6.5 and the best performance for PV model by having tags on right shoulder is when $\sigma_a = 1$, as shown in Figure 6.6 and Table 6.4.

Performance	
2DLocErr	[avg=0.178, std=0.104, RMS=0.207] m
3DLocErr	[avg=0.420, std=0.094, RMS=0.430] m
xErr	[avg=0.053, std=0.072, RMS=0.090] m
yErr	[avg=0.150, std=0.111, RMS=0.186] m
zErr	[avg=-0.335, std=0.173, RMS=0.193] m

Table 6.4: 3 Tags - Performance of σ_a for PV model

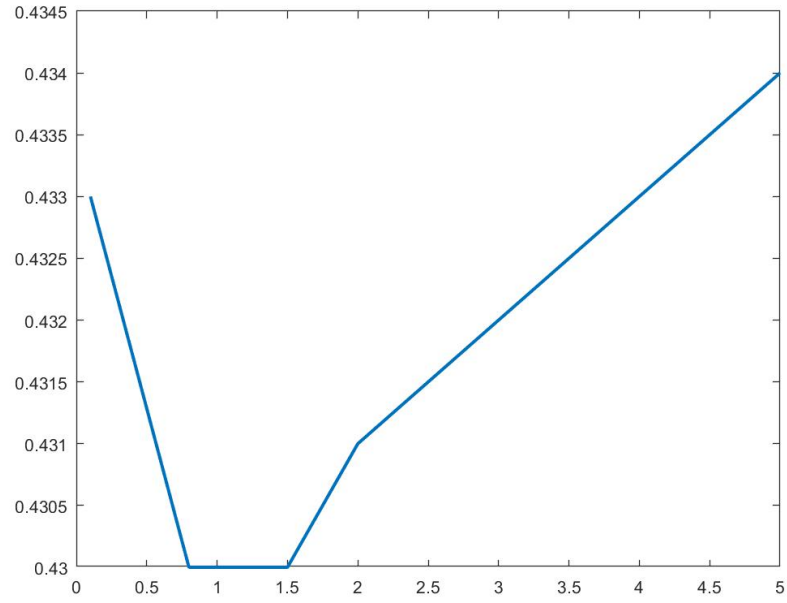


Figure 6.5: Ratio between σ_a and rmse as a function of σ_a

F₃Tags, 2DLocErr [avg=0.178, std=0.104, rmse=0.207] m - 3DLocErr [avg=0.420, std=0.094, rmse=0.430] m - XErr [avg=0.053, std=0.072, rmse=0.090] m - YErr [avg=0.150, std=0.111, rmse=0.186] m - ZErr [avg=-0.335, std=0.173, rmse=0.335] m

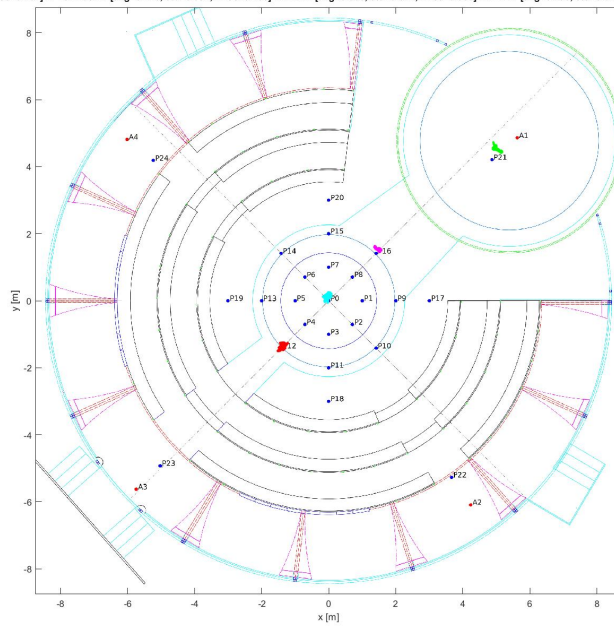


Figure 6.6: PV model - 3 Tags on back belt

Chapter 7

Performance Comparisons and Conclusions

7.1 Performance Comparisons

By evaluating ranging measurement for different number of tags on right shoulder, right pocket and back belt the range of errors can be estimated.

As shown in Table 7.1, the best performance for P model and PV model for different number of tags on right shoulder are shown

The best performance is when there are 2 tags on right shoulder for p model, as shown in Table 7.1

1 Tag / σ_a / rmse	P model / 0.01 / 0.667
1 Tag / σ_a / rmse	PV model / 1.5 / 0.731
2 Tags / σ_a / rmse	P model / 0.5 / 0.107
2 Tags / σ_a / rmse	PV model / 0.01 / 0.109
3 Tags / σ_a / rmse	P model / 3.5 / 0.134
3 Tags / σ_a / rmse	PV model / 3 / 0.137

Table 7.1: Comparison effect of human body on UWB signal by having different number of Tags

7.2 Conclusions

This thesis presents design and implementation of a UWB 3-D localization system for real time augmented reality applications to be applied in TV studios. It first

presents the state of art of RTLS based on the UWB technology. After that, it focuses on the design of the RTLS.

The UWB-based Localization System is formed by the Anchors and the Tags. In a real-time location system (RTLS), anchors are electronic devices that detect UWB pulses emitted by UWB Tags and forward them to the location server for calculating tag positions. Tags are small electronic devices that are attached to objects that need to be tracked. These devices exchange range messages and send in real-time the range measurements to a gateway where a localization algorithm, based on EKF, runs to estimate tag's position according to a relative references system.

In this thesis, to evaluate the performance of the designed EKF algorithm, 25 test points have been chosen for the tag's position and the localization algorithm has been tested via Matlab simulation in an indoor area where 8 anchors have been deployed. The measurement campaign has been carried out in RAI by using UWB devices from synchronicIT. These measurements were done in different scenarios without obstacle and with human body, as shown in Figure 7.1.

Ranging and localization error statics have been calculated by using the formulas shown in figure 7.2. Then for getting better Precision and accuracy, we take into account these error statics for obtaining value of mean, standard deviation and RMS.

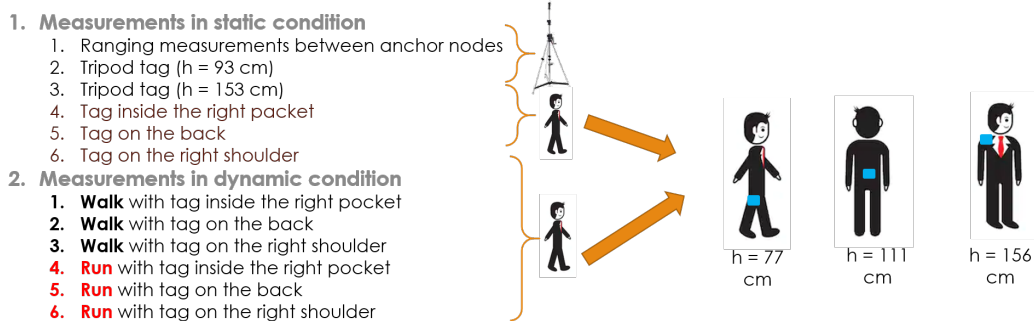


Figure 7.1: Measurements Scenarios

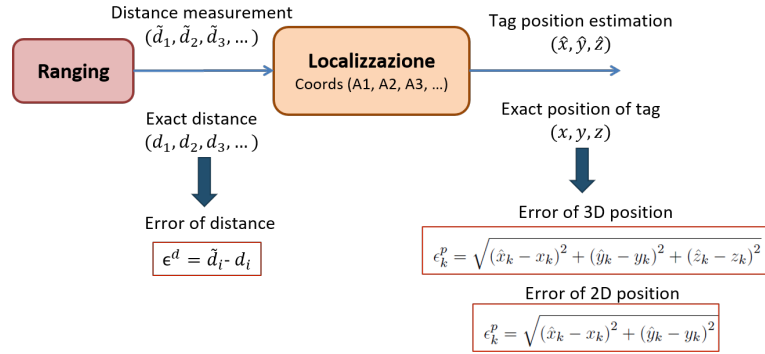


Figure 7.2: Ranging and Location Statistics

The positioning phase was used the extended Kalman filter (EKF) since it is robust and smaller complex than many others algorithms. Generating of EKF filter and state models were done by Matlab. In this thesis, EKF is simulated to show its features and how its parameters change the tracking performance by using two different state namely, Position (P) model and Position velocity (PV) model. Several tests were done in order to evaluate and compare different localization performance without obstacle and with human body.

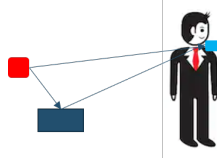


Figure 7.3: The Multi-Path effect in the presence of the human body

Due to human body interference, sometimes the direct path is obstructed and the receiver synchronizes on a reflected path, thus affecting the range measurement, as shown in Figure 7.3.

Different tests were performed in RAI TV studio by using EKF algorithm for different tags. In this thesis, first of all performance evaluation by 1 tag to find the best σ (which is one of parameters of Q matrix) that minimise the 3DLoc error rmse for two state models, P model and PV model. Then this simulation has been continued by having 2 tags and 3 tags on the right shoulder to see how performance will be changed, as shown in Table 7.1.

By comparing 1 tag, 2 tags and 3 tags, It shows for 1 tag on right shoulder the number of errors are more and by comparing P model and PV model, we recognize value of σ is smaller for P model. So, when we have 1 tag on right shoulder, P model has best performance and smaller number of errors comparing with PV model.

By have 2 tags on right shoulder for P model, we have smaller number of errors, however the value of σ increased comparing with case when we have only 1 tag. So when we have 2 tags still P model has best performance. Number of errors for both P model is less than PV and value of σ for PV model is less than P model. so, when we have 3 tags, it's better to use P model as data are less spread out. As result, among these 3 cases, for having the best performance, it's better to use 2 tags on right shoulder by using P model, as shown in Figure 7.4, and after that using 3 tags on right shoulder for P model can be considered as second choice.



Figure 7.4: Using 2 tags on right shoulder as best performance

Appendix

.1 Main code

Part of main code which consist of test points and different cases of right shoulder, right pocket and back belt which in this thesis evaluated.

```
1 %swTagPos = 'right_shoulder';
2 %swTagPos = 'right_pocket';
3 swTagPos = 'back_belt';
4 disp(['Alg: ', nameAlg]);
5 numMaxRangeInitLoc = 5; % within the first numMaxRangeInitLoc sets of
   range measurements —> take the minimum range
6 swFiltCoord = 1; % use the Tings algorithm to filter the estimated
   coordinates
7 %Exact coordinates of test points
8 testPoints = [
9     0,          0,          0;          %0
10    1,          0,          0;          %1
11    0.7071,    -0.7071,    0;          %2
12    0,         -1,          0;          %3
13   -0.7071,   -0.7071,    0;          %4
14   -1,         0,          0;          %5
15   -0.7071,    0.7071,    0;          %6
16    0,         1,          0;          %7
17    0.7071,    0.7071,    0;          %8
18    2,         0,          0;          %9
19    1.4142,   -1.4142,    0;          %10
20    0,         -2,          0;          %11
21   -1.4142,   -1.4142,    0;          %12
22   -2,         0,          0;          %13
23   -1.4142,    1.4142,    0;          %14
24    0,         2,          0;          %15
25    1.4142,    1.4142,    0;          %16
26    3,         0,          0;          %17
27    0,        -3,          0;          %18
28   -3,         0,          0;          %19
```

```

29 0,          3,          0;          %20
30 4.864,     4.207,     0.392;     %21
31 3.661,     -5.268,    0.72;     %22
32 -5.02,     -4.924,    0.72;     %23
33 -5.227,    4.137,     0.72];    %24
34
35     end

```

.2 P model and PV model for 3 Tags

Part of Matlab algorithm for P model and PV model in case of 3Tags.

```

1  if (ekfStruct.model == 0)
2      ekfStruct.state = [coordTag1InitialEst(1:dim)'
3      coordTag2InitialEst(1:dim)' coordTag3InitialEst(1:dim)']; % [x1,
4      y1, z1, x2, y2, z2]
5      ekfStruct.F = eye(3*dim);
6      ekfStruct.Q = (Delta* eye(3*dim))*(Delta * eye(3*dim))' * sigmaA
7      ^ 2;
8      if (swInputPmatrix == 1)
9          ekfStruct.P = [P1, zeros(dim), zeros(dim); zeros(dim), P2, zeros(
10         dim); zeros(dim), zeros(dim), P3];
11         elseif (swInputPmatrix == 0)
12             ekfStruct.P = [sigmax1^2, 0, 0, 0, 0, 0, 0, 0, 0;
13                 0, sigmay1^2, 0, 0, 0, 0, 0, 0, 0;
14                 0, 0, sigmaz1^2, 0, 0, 0, 0, 0, 0;
15                 0, 0, 0, sigmax2^2, 0, 0, 0, 0, 0;
16                 0, 0, 0, 0, sigmay2^2, 0, 0, 0, 0;
17                 0, 0, 0, 0, 0, sigmaz2^2, 0, 0, 0;
18                 0, 0, 0, 0, 0, 0, sigmax3^2, 0, 0;
19                 0, 0, 0, 0, 0, 0, 0, sigmay3^2, 0;
20                 0, 0, 0, 0, 0, 0, 0, 0, sigmaz3^2];
21         end
22         elseif (ekfStruct.model == 1)
23             ekfStruct.state = [coordTag1InitialEst(1:dim)'
24             coordTag2InitialEst(1:dim)' coordTag3InitialEst(1:dim)' 0 0 0 0 0
25             0 0 0 0];
26             ekfStruct.F = [eye(3*dim), Delta*eye(3*dim); zeros(3*dim), eye(3*
27             dim)];
28             ekfStruct.Q = [ Delta^2*eye(3*dim)/2 ; Delta*eye(3*dim)]*[ Delta
29             ^2*eye(3*dim)/2 ; Delta*eye(3*dim)]' * sigmaA^2;
30         end

```

.3 EKF for 3 Tags

Part of Matlab algorithm for generating EKF for 3Tags

```

1 Q = ekfStruct.Q;
2   P = F * P * F' + Q;
3   Z = [Z1; Z2; Z3];
4   numMeas = length(Z);
5   if (numMeas >= 4)
6       estimated = 1;
7   else
8       estimated = 0;
9   end
10  h1 = sqrt((x1Tag-x1Ref).^2+(y1Tag-y1Ref).^2+(z1Tag-z1Ref).^2);
11  h2 = sqrt((x2Tag-x2Ref).^2+(y2Tag-y2Ref).^2+(z2Tag-z2Ref).^2);
12  h3 = sqrt((x3Tag-x3Ref).^2+(y3Tag-y3Ref).^2+(z3Tag-z3Ref).^2);
13  h = [h1; h2; h3];
14  numMeas1 = length(h1);
15  numMeas2 = length(h2);
16  numMeas3 = length(h3);
17  if (model == 0)
18      H = [(x1Tag-x1Ref)./h1, (y1Tag-y1Ref)./h1, (z1Tag-z1Ref)./h1,
19          zeros(numMeas1,6),
20          zeros(numMeas2,3), (x2Tag-x2Ref)./h2, (y2Tag-y2Ref)./h2, (
21          z2Tag-z2Ref)./h2, zeros(numMeas2,3);
22          zeros(numMeas3,6), (x3Tag-x3Ref)./h3, (y3Tag-y3Ref)./h3, (
23          z3Tag-z3Ref)./h3];
24  else
25      H = [(x1Tag-x1Ref)./h1, (y1Tag-y1Ref)./h1, (z1Tag-z1Ref)./h1,
26          zeros(numMeas1,15);
27          zeros(numMeas2,3), (x2Tag-x2Ref)./h2, (y2Tag-y2Ref)./h2, (
28          z2Tag-z2Ref)./h2, zeros(numMeas2,12);
29          zeros(numMeas3,6), (x3Tag-x3Ref)./h3, (y3Tag-y3Ref)./h3, (
30          z3Tag-z3Ref)./h3, zeros(numMeas3,9)];
31  end
32  R = eye(numMeas) * sigmaDist^2;
33  s = Z - h;
34  S = (H*P*H') + R;
35  K = P * H' * S;
36  n = length(ekfStruct.state);
37  I = eye(n);
38  x = x + (K * s);
39  P = (I - (K * H)) * P;
40  ekfStruct.state = x';
41  ekfStruct.P = P;
42 end

```

Bibliography

- [1] Chris Gkiokas "*Localization of a Mobile Node in a Wireless Sensor Network: an Evaluation of RSSI as a Distance Metric*". 26 April 2015
- [2] Dr. Brian Gaffney.
"Considerations and challenges in real time locating systems design.". De-cawave Ltd, 2014..
- [3] Mario Alexander Ruiz Guirales. "*Design and Implementation of a Cooperative Indoor Localization System based on UWB Devices*". Politecnico di Torino. 2016.
- [4] Mauricio A. Caceres, Francesco Sottile, and Maurizio A. Spirito. "*Adaptative Location Tracking by Kalman Filter in Wireless Sensor Networks*". Proc. IEEE International Conferences On Wireless and Mobile Computing, Networking and Communications, pp. 123-128,2009.
- [5] M. R. Gholami, S. Gezici, E. G. Ström, M. Rydström. *Positioning algorithms for cooperative networks 340 in the presence of an unknown turn-around time*. SPAWC, 2011, pp. 166–170.
- [6] Guenther Retscher, Vassilis Gikas, Hannes Hofer, Harris Perakis, Allison Kealy *Range validation of UWB and Wi-Fi for integrated indoor positioning*. 15 January 2019
- [7] C. Cook, Radar signals *An introduction to theory and application*. Elsevier Science, 2012
- [8] Orlando Tovar, "*Design and Implementation of an Indoor Localization System based on IEEE 802.15.4a Devices*," 2014.
- [9] M. Dai "*Design of Cognitive Tracking Algorithms Based on Wireless Technologies*"September, 2012.
- [10] M. A. Caceres, F. Sottile, and M. A. Spirito, "*Adaptive Location Tracking by Kalman Filter in Wireless Sensor Networks*," *IEEE International Conference on Wireless and Mobile Computing, Networking and Communications* 2009.